




An Adaptive and Quasi-periodic HDG Method for Maxwell's Equations in Heterogeneous Media

Liliana Camargo¹ · Bibiana López-Rodríguez² · Mauricio Osorio²  · Manuel Solano^{3,4}

Received: 8 November 2022 / Revised: 16 March 2023 / Accepted: 22 September 2023 /
Published online: 22 November 2023
© The Author(s) 2023

Abstract

With the aim to continue developing a hybridizable discontinuous Galerkin (HDG) method for problems arisen from photovoltaic cells modeling, in this manuscript we consider the time harmonic Maxwell's equations in an inhomogeneous bounded bi-periodic domain with quasi-periodic conditions on part of the boundary. We propose an HDG scheme where quasi-periodic boundary conditions are imposed on the numerical trace space. Under regularity assumptions and a proper choice of the stabilization parameter, we prove that the approximations of the electric and magnetic fields converge, in the L^2 -norm, to the exact solution with order h^{k+1} and $h^{k+1/2}$, resp., where h is the meshsize and k the polynomial degree of the discrete spaces. Although, numerical evidence suggests optimal order of convergence for both variables. An *a posteriori* error estimator for an energy norm is also proposed. We show that it is reliable and locally efficient under certain conditions. Numerical examples are provided to illustrate the performance of the quasi-periodic HDG method and the adaptive scheme based on the proposed error indicator.

✉ Mauricio Osorio
maosorio@unal.edu.co

Liliana Camargo
limcamargoma@unal.edu.co

Bibiana López-Rodríguez
blopezz@unal.edu.co

Manuel Solano
msolano@ing-mat.udec.cl

¹ Grupo de Investigación Computación Científica, Universidad Nacional de Colombia, Sede Medellín, Colombia

² Escuela de Matemáticas, Universidad Nacional de Colombia, Sede Medellín, Colombia

³ Departamento de Ingeniería Matemática, Facultad de Ciencias Físicas y Matemáticas, Universidad de Concepción, Concepción, Chile

⁴ Centro de Investigación en Ingeniería Matemática (CI2MA), Universidad de Concepción, Concepción, Chile

Keywords A posteriori error · Hybridizable discontinuous Galerkin method · Time-harmonic · Maxwell's equations · Quasi-periodic conditions · Heterogeneous media

Mathematics Subject Classification 65N12 · 65N15

1 Introduction

Photovoltaic cells have been intensively studied in nanoscience and nanotechnology researches, due to the possibility of obtaining electrical energy from the sunlight, which is considered as a green energy choice. This renewable resource of energy can be used in place of fossil fuels, in order to achieve lower harmful emissions into the atmosphere, a reduced carbon footprint and fewer air pollutants.

For some decades, the search of new sustainable sources of electrical energy has encouraged projects whose main goals consist on improving the capability to collect sunlight of the photovoltaic cells with periodic surface-relief gratings and increasing the electrical energy generation. In fact, one of the strategies to increase the efficiency of light harvesting by solar cells, is the use of plasmonic structures that enhance the intensity of the electromagnetic field [32]. The key idea is to texture the surface of the metallic back-reflector of a thin-film solar cell by periodic corrugations of size proportional to the wavelength. Under some conditions [32], this configuration produces an excitation of the electrons placed on the surface of the metal, generating a wave that propagates through the surface called surface plasmon polariton (SPP) wave. For instance, this occurs when the propagation constant β^{SPP} of a SPP wave and the propagation constant β^{inc} of the incident wave satisfy $\beta^{\text{SPP}} = \beta^{\text{inc}} + 2n\pi$, for some $n \in \mathbb{Z}$ in the transverse magnetic (TM) polarization, see Sections 2.1 and 2.2 of [32]. In the same direction, multiple SPP waves can be generated by placing a periodic multi-layered isotropic dielectric material on top of the metallic back-reflector [19]. Furthermore, structures involving different type of materials have been considered in order to optimize the performance of the cells, see for example [46] and references therein. In those cases, it is possible to maximize the spectrally averaged electron hole pair density and the solar-spectrum-integrated power-flux density [4, 19, 37, 45]. This optimization process is expensive from the computational point of view since the functionals to maximize depend on the solution to Maxwell's equations and also on geometric and optical parameters. This fact motivates the development and analysis of new methods able to reduce the computational costs. In this regard, some authors have used numerical techniques in order to state and approximate the solution of boundary value problems, in which the effect of unpolarized or polarized incident plane waves on the surface of the cell and a wide range of geometrical and optical parameters in the frequency-domain Maxwell's equations, have been considered. Among them, we highlight the exact modal method [23], the moment method (MoM) [33], the rigorous coupled-wave approach (RCWA) [37, 46], the finite-difference time-domain (FDTD) method [27], the finite element method (FEM) [5, 26, 35, 36, 42, 46], and hybridizable discontinuous Galerkin (HDG) methods [10, 11, 13, 14, 20, 39, 47]. We focus our study on the latter.

Perhaps, from the numerical analysis point of view, three main challenges arise from the model: the complex-valued electric permittivity, the quasi-periodic boundary condition and the outgoing radiation condition above and below the solar cell structure. Most of the known studies assume a positive electric permittivity and consider prescribed boundary data. Under that assumption, in [20] an HDG method to study the three-dimensional time harmonic

Maxwell's equations coupled with the impedance boundary condition was proposed, in the case of high wave numbers. The stability and error estimates for the method were deduced by employing the constraint $\kappa h \leq 1$. Based on the reliable results showed in the above work and in [14, 39], some authors considered complex-valued permittivities [10, 35, 47] and not perfect conducting boundary conditions. More precisely, in [47] a high-order HDG scheme for Maxwell's equations augmented with the hydrodynamic model, for the conduction-band electrons in noble metals, is stated. The radiation conditions can be handled by boundary element methods [24], absorbing boundary conditions (ABCs) [38], Dirichlet-to-Neumann (DtN) techniques, based on Fourier expansions [1] and by the perfectly matched layer (PML) technique, [8, 15, 41].

Inspired in the application described above, in this work we consider a problem in which the time harmonic Maxwell's equations are defined in a bounded domain $\Omega \subset \mathbb{R}^3$ occupied by one period of a bi-periodic structure, illuminated by an incident electromagnetic wave. Our heterogeneous domain Ω corresponds to the disjoint union between the region Ω_d , occupied by an isotropic dielectric material with positive real relative permittivity and a metallic region denoted Ω_m , whose relative permittivity is a complex-valued number with negative real part, see [10]. On the top and bottom boundaries of the unit cell, we consider Dirichlet type conditions and impose quasi-periodic conditions on the vertical walls of Ω . Quasi-periodic conditions can be added to the system of equations defined in symmetric or asymmetric domains with periodic characteristics, see Sections 3.1 and 3.3 of [26] and Section 2 of [48]. These kind of boundary conditions differ by a complex exponential factor or Bloch phase, on the parallel walls of the domain. In order to carry out an a priori error analysis of our 3D problem subjected to Dirichlet and quasi-periodic conditions, we based on the analysis developed in [10]. Even though we are not considering exactly the original model since we impose Dirichlet boundary condition at the top and bottom walls instead of dealing with the outgoing radiation condition, this "simplified" problem poses several challenges that must be addressed first. Therefore, we consider the analysis that we will present in this manuscript constitutes as a key stepping stone towards the goal of studying the full model.

On the other hand, the change of material across the non-smooth metallic interface, might produce singularities near the corners. Moreover, as previously discussed, the magnitude of electromagnetic field is high near the metal surface due to the plasmonic effect. Therefore, in that region, the finite element mesh must be fine enough to capture this phenomena accurately. This can be efficiently achieved by an adaptive scheme able detect where to localize the mesh refinement based on an error indicator.

In the case of an *a posteriori* error indicator for Maxwell's equations, one of the main challenges are the non-coercivity of the bilinear form and the low regularity of the exact solution. Residual based *a posteriori* error estimates for Maxwell's equations in electromagnetic scattering problems were introduced in [7, 34]. The author in [34] showed how an *a posteriori* error indicator can be derived using an adjoint equation approach and also the fact that there is a limit on the maximum diameter of the elements in a grid, imposed by the non-coercivity of the bilinear form. Later, [43] proved the reliability of the residual error estimators on Lipschitz domains, which had been proposed and analyzed in [7]. In [28], the authors derived an *hp*-type *a posteriori* error estimate for the time-harmonic Maxwell's equations and, in [31], carried out an *a posteriori* error analysis for the time-dependent Maxwell's equations. For the steady state coercive Maxwell's equations, the authors in [13] provided a computable residual-based *a posteriori* error estimator, which is independent of the regularity parameter of the solution and it is based on the error measured in terms of a mesh-dependent energy norm. On the other hand, by using hierarchical basis, [6] proposed a hierarchical error estimator for quasi-magnetostatic eddy current problem discretized by

means of lowest order curl-conforming finite elements on tetrahedral meshes. They provided a saturation assumption in order to guarantee the reliability and efficiency of the estimator.

In this manuscript, we extend the residual-based *a posteriori* error estimator for the coercive Maxwell's equations, developed in [13]. We will establish reliability and local efficiency of the error estimator proposed for our HDG scheme, by using approximation properties of continuous functions, Helmholtz decompositions, the Scott-Zhang interpolation operator and a standard localization technique, based on element and face bubble functions [2]. Moreover, in the context of discontinuous Galerkin methods, it is crucial the use of a continuous approximation of a discontinuous piece-wise polynomial function [29, 30], sometimes called Oswald interpolant inspired in the work by [40] for piecewise linear approximations. This interpolant has been employed in the deduction of *a posteriori* error estimators for HDG methods [3, 12, 16, 17]. In our case, we modify this operator in such a way that it preserves quasi-periodic boundary conditions (see Appendix A.2).

The rest of this paper is organized as follows. In Sect. 2 we define the truncated domain and introduce the boundary value problem. In Sect. 3, we propose an HDG method and prove it is well posed. Then, we briefly describe the stability analysis and the error analysis for the method. The residual-based *a posteriori* error estimator for our HDG method is developed and analyzed in the fourth section. Finally, in Sect. 5 we show some numerical results by using uniform refined meshes and adaptive refined meshes.

2 Problem Statement

Through the manuscript we will use standard simplified terminology for Sobolev spaces and norms, where vector-valued functions are bold-faced. In particular, if \mathcal{O} is a domain in \mathbb{R}^3 , Σ is an open or closed Lipschitz surface, and $s \in \mathbb{R}$, we set $\mathbf{H}^s(\mathcal{O}) := [\mathbf{H}^s(\mathcal{O})]^3$, $\mathbf{H}^s(\Sigma) := [\mathbf{H}^s(\Sigma)]^3$ and their corresponding norms $\|\cdot\|_{s,\mathcal{O}}$ for $\mathbf{H}^s(\mathcal{O})$ and $\mathbf{H}^s(\Sigma)$; and $\|\cdot\|_{s,\Sigma}$ for $\mathbf{H}^s(\Sigma)$ and $\mathbf{H}^s(\Sigma)$. In the case $s = 0$, we write $\mathbf{L}^2(\mathcal{O})$, $\mathbf{L}^2(\Sigma)$ and $\mathbf{L}^2(\Sigma)$ instead of $\mathbf{H}^0(\mathcal{O})$, $\mathbf{H}^0(\mathcal{O})$, $\mathbf{H}^0(\Sigma)$ and $\mathbf{H}^0(\Sigma)$, respectively; and in the notation for their norms, the first subindex will not be included. For $s > 0$, we write $|\cdot|_{s,\mathcal{O}}$ for the \mathbf{H}^s - and \mathbf{H}^s -seminorms. From ahead, $\mathbb{P}_k(\mathcal{O})$ denotes the space of complex-valued polynomials of degree less or equal than $k \geq 0$, $\mathbf{P}_k(\mathcal{O}) := [\mathbb{P}_k(\mathcal{O})]^3$ and by $(\cdot, \cdot)_{\mathcal{O}}$ and $(\cdot, \cdot)_{\partial\mathcal{O}}$, we denote the $\mathbf{L}^2(\mathcal{O})$ and $\mathbf{L}^2(\partial\mathcal{O})$ inner products, respectively.

In addition, we introduce the following spaces

$$\begin{aligned} \mathbf{H}(\operatorname{div}_{\epsilon}; \mathcal{O}) &:= \{\mathbf{w} \in \mathbf{L}^2(\mathcal{O}) : \nabla \cdot (\epsilon \mathbf{w}) \in \mathbf{L}^2(\mathcal{O})\}, \\ \mathbf{H}(\operatorname{div}_{\epsilon}^0; \mathcal{O}) &:= \{\mathbf{w} \in \mathbf{L}^2(\mathcal{O}) : \nabla \cdot (\epsilon \mathbf{w}) = 0\}, \\ \mathbf{H}_0(\operatorname{div}; \mathcal{O}) &:= \{\mathbf{w} \in \mathbf{H}(\operatorname{div}; \mathcal{O}) : \mathbf{w} \cdot \mathbf{n}|_{\partial\mathcal{O}} = 0\}, \\ \mathbf{H}_{\vartheta}(\operatorname{div}; \mathcal{O}) &:= \{\mathbf{w} \in \mathbf{H}(\operatorname{div}; \mathcal{O}) : \mathbf{w} \cdot \mathbf{n}|_{\vartheta} = 0\}, \\ \mathbf{H}(\operatorname{curl}; \mathcal{O}) &:= \{\mathbf{w} \in \mathbf{L}^2(\mathcal{O}) : \nabla \times \mathbf{w} \in \mathbf{L}^2(\mathcal{O})\}, \\ \mathbf{H}_0(\operatorname{curl}; \mathcal{O}) &:= \{\mathbf{w} \in \mathbf{H}(\operatorname{curl}; \mathcal{O}) : \mathbf{w} \times \mathbf{n}|_{\partial\mathcal{O}} = 0\}, \\ \mathbf{H}_{\vartheta}(\operatorname{curl}; \mathcal{O}) &:= \{\mathbf{w} \in \mathbf{H}(\operatorname{curl}; \mathcal{O}) : \mathbf{w} \times \mathbf{n}|_{\vartheta} = 0\}, \end{aligned}$$

where $\vartheta \subset \partial\mathcal{O}$ and \mathbf{n} denotes the outward unit normal vector to $\partial\mathcal{O}$. For a vector-valued function \mathbf{w} defined on a face F , we denote by $\mathbf{w}^t := (\mathbf{n} \times \mathbf{w}) \times \mathbf{n}$ and $\mathbf{w}^n := (\mathbf{w} \cdot \mathbf{n})\mathbf{n}$ its tangential and normal components, respectively. It follows that $\mathbf{w} := \mathbf{w}^t + \mathbf{w}^n$ and $\mathbf{w}^t \times \mathbf{n} = \mathbf{w} \times \mathbf{n}$.

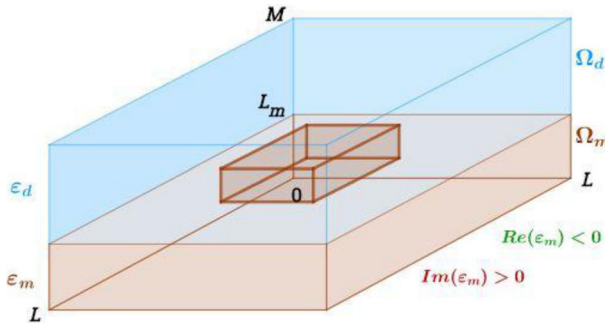


Fig. 1 Example of a domain Ω : a dielectric region Ω_d placed on top of a metallic backreflector Ω_m

Furthermore, to avoid proliferation of unimportant constants, the expression $A \leq CB$, for some $C > 0$ independent of the meshsize, will be replaced by $A \lesssim B$.

Now, let us characterize our simply connected domain $\Omega := (0, L) \times (0, L) \times (0, M)$, with $L, M > 0$ with polyhedral connected boundary $\Gamma := \Gamma_1 \cup \Gamma_2 \cup \Gamma_3 \cup \Gamma_4 \cup \Gamma_B \cup \Gamma_T$. Here,

$$\begin{aligned} \Gamma_1 &:= \{(0, y, z) : y \in (0, L), z \in (0, M)\}, & \Gamma_2 &:= \{(L, y, z) : y \in (0, L), z \in (0, M)\}, \\ \Gamma_3 &:= \{(x, 0, z) : x \in (0, L), z \in (0, M)\}, & \Gamma_4 &:= \{(x, L, z) : x \in (0, L), z \in (0, M)\}, \\ \Gamma_B &:= \{(x, y, 0) : x \in (0, L), y \in (0, L)\}, & \Gamma_T &:= \{(x, y, M) : x \in (0, L), y \in (0, L)\}. \end{aligned}$$

In applications arising from solar cell modeling, Ω corresponds to one period of a bi-periodic array, where the unit cells are joined through quasi-periodic boundary conditions, which are imposed on the vertical walls of Ω , Γ_1 - Γ_2 and Γ_3 - Γ_4 . In this phenomenon, after the sunlight illuminates the top boundary Γ_T , outgoing and evanescent waves are generated, below the bottom boundary Γ_B and above Γ_T , as well. In this work we assume that the data on Γ_B and Γ_T are prescribed, but we consider quasi-periodic boundary conditions on Γ_1 - Γ_2 and Γ_3 - Γ_4 .

The domain Ω is divided in two subdomains. A dielectric region Ω_d with permittivity $\epsilon_d \in \mathbb{R}^+$ and a metallic region Ω_m with electric permittivity $\epsilon_m \in \mathbb{C}$, satisfying $\text{Re}(\epsilon_m) < 0$ and $\text{Im}(\epsilon_m) > 0$, as it was shown in Fig. 1.

Given $\mathbf{J} \in \mathbf{H}(\text{div}^0; \Omega)$ and $\hat{\mathbf{g}} \in \gamma_t(\mathbf{H}(\mathbf{curl}; \Omega) \cap \mathbf{H}(\text{div}^0_\epsilon; \Omega))$, where γ_t denotes the tangential trace operator, we look for \mathbf{E} and \mathbf{H} such that

$$\nabla \times \mathbf{E} = i \omega \mu_0 \mathbf{H}, \quad \text{in } \Omega, \tag{1a}$$

$$\nabla \times \mathbf{H} = \mathbf{J} - i \omega \epsilon_0 \mathbf{E}, \quad \text{in } \Omega, \tag{1b}$$

$$\mathbf{E} \times \mathbf{n} = \hat{\mathbf{g}}, \quad \text{on } \Gamma_B \cup \Gamma_T, \tag{1c}$$

$$\mathbf{E}(L, y, z) = e^{i\alpha L} \mathbf{E}(0, y, z), \quad y \in (0, L), z \in (0, M), \tag{1d}$$

$$\mathbf{E}(x, L, z) = e^{i\beta L} \mathbf{E}(x, 0, z), \quad x \in (0, L), z \in (0, M), \tag{1e}$$

where \mathbf{E} denotes the electric field, \mathbf{H} the magnetic field and \mathbf{J} the current density, which satisfy an implicit $e^{-i\omega t}$ dependence of time at frequency $\omega > 0$. The other parameters are the permeability of free space μ_0 , the electric permittivity of free space ϵ_0 , the electric permittivity ϵ , the relative permittivity $\epsilon_0\epsilon$, the free-space wavenumber $\kappa := \omega\sqrt{\epsilon_0\mu_0}$, the free-space wavelength $\lambda_0 := 2\pi/\kappa$ and the intrinsic impedance of the free space $\eta_0 := \sqrt{\mu_0/\epsilon_0}$. Furthermore, $\mu_0 = 4\pi \times 10^{-7} \text{ Hm}^{-1}$, $\epsilon_0 = 8.854 \times 10^{-12} \text{ Fm}^{-1}$, \mathbf{n} denotes the outward unit normal to Γ and the permittivity is defined as $\epsilon = \epsilon_m$ in Ω_m and $\epsilon = \epsilon_d$ in Ω_d . According

to the theory that appears in Section 1.3 of [35], the solutions of (1) exist and have the form of a plane wave. A plane wave is defined as an electromagnetic wave whose polarization, \mathbf{A} , satisfies the property $\mathbf{A} \cdot (\alpha, \beta, \gamma) = 0$, for $\alpha := \kappa \sin \theta \cos \phi$, $\beta := \kappa \sin \theta \sin \phi$ and $\gamma := \kappa \cos \theta$, with $\theta \in [0, \pi]$ and $\phi \in [0, 2\pi]$. Based on the form of the solutions it is possible to characterize the *quasi-periodic boundary conditions*, which in this problem were added by the Eqs. (1d) and (1e).

Let us introduce in (1) the change of variable $\mathbf{u} := \epsilon_0^{1/2} \mathbf{E}$, $\mathbf{v} := i\kappa\mu_0^{1/2} \mathbf{H}$. By a Lagrange multiplier p , we impose the incompressibility condition $\nabla \cdot (\epsilon \mathbf{E}) = 0$, which can be deduced from the second equation. For a more detailed description of (1), we refer to [35]. Then, we obtain the following problem: Find \mathbf{u} , \mathbf{v} and p such that

$$\mathbf{v} - \nabla \times \mathbf{u} = 0, \quad \text{in } \Omega, \tag{2a}$$

$$\nabla \times \mathbf{v} - \kappa^2 \epsilon \mathbf{u} + \bar{\epsilon} \nabla p = \mathbf{f}, \quad \text{in } \Omega, \tag{2b}$$

$$\nabla \cdot (\epsilon \mathbf{u}) = 0, \quad \text{in } \Omega, \tag{2c}$$

$$\mathbf{u} \times \mathbf{n} = \mathbf{g}, \quad \text{on } \Gamma_B \cup \Gamma_T, \tag{2d}$$

$$\mathbf{u}(L, y, z) = e^{i\alpha L} \mathbf{u}(0, y, z), \quad y \in (0, L), z \in (0, M), \tag{2e}$$

$$\mathbf{u}(x, L, z) = e^{i\beta L} \mathbf{u}(x, 0, z), \quad x \in (0, L), z \in (0, M), \tag{2f}$$

$$p = 0, \quad \text{on } \Gamma, \tag{2g}$$

where $\mathbf{f} := i\kappa\mu_0^{1/2} \mathbf{J}$, $\mathbf{g} := \epsilon_0^{1/2} \hat{\mathbf{g}}$ and $\bar{\epsilon}$ is the complex conjugate of ϵ . In order to simplify notation, we define $\Gamma_0 := \Gamma_B \cup \Gamma_T$ and $\Gamma_{QP} := \Gamma_1 \cup \Gamma_2 \cup \Gamma_3 \cup \Gamma_4$.

Now, let us introduce the spaces

$$H^{QP}(\mathbf{curl}; \Omega) := \left\{ \mathbf{w} \in H(\mathbf{curl}; \Omega) : \mathbf{w}|_{\Gamma_2} = e^{i\alpha L} \mathbf{w}|_{\Gamma_1}, \mathbf{w}|_{\Gamma_4} = e^{i\beta L} \mathbf{w}|_{\Gamma_3} \right\},$$

$$H_{\Gamma_0}^{QP}(\mathbf{curl}; \Omega) := \left\{ \mathbf{w} \in H^{QP}(\mathbf{curl}; \Omega) : \mathbf{w} \times \mathbf{n}|_{\Gamma_0} = 0 \right\},$$

$$\mathbf{X}_{QP} := H_{\Gamma_0}^{QP}(\mathbf{curl}; \Omega) \cap H(\text{div}_\epsilon^0; \Omega),$$

$$\mathbf{X}_{QP}^{\mathbf{g}} := \left\{ \mathbf{w} \in H^{QP}(\mathbf{curl}; \Omega) \cap H(\text{div}_\epsilon^0; \Omega) : \mathbf{w} \times \mathbf{n}|_{\Gamma_0} = \mathbf{g} \right\},$$

endowed with the $H(\mathbf{curl}; \Omega)$ -norm, $\|\mathbf{w}\|_{H(\mathbf{curl}; \Omega)} := (\|\mathbf{w}\|_\Omega^2 + \|\nabla \times \mathbf{w}\|_\Omega^2)^{1/2}$. With respect to the existence and uniqueness of the solutions of (2), we have the following Lemma.

Lemma 1 *If $\kappa^2 \epsilon_d$ is not an eigenvalue of $\nabla \times \nabla \times$ in Ω_d , then (2) has a unique solution $(\mathbf{v}, \mathbf{u}, p) \in H(\mathbf{curl}; \Omega) \times \mathbf{X}_{QP}^{\mathbf{g}} \times H_0^1(\Omega)$.*

Proof By tailoring the proofs showed in Section 5 of [9], we can guarantee the existence of a unique solution, when $\mathbf{g} = \mathbf{0}$, for the following variational formulation: Find $(\mathbf{u}, p) \in \mathbf{X}_{QP} \times H_0^1(\Omega)$ such that

$$\begin{aligned} (\nabla \times \mathbf{u}, \nabla \times \mathbf{w})_\Omega - \kappa^2 (\epsilon \mathbf{u}, \mathbf{w})_\Omega &= (\mathbf{f}, \mathbf{w})_\Omega, \\ (\bar{\epsilon} \nabla p, \nabla q)_\Omega &= (\mathbf{f}, \nabla q)_\Omega, \end{aligned} \tag{3}$$

for all $(\mathbf{w}, q) \in \mathbf{X}_{QP} \times H_0^1(\Omega)$.

In the case $\mathbf{g} \neq \mathbf{0}$, we have that if $\mathbf{g} \in \gamma_t(H(\mathbf{curl}; \Omega) \cap H(\text{div}_\epsilon^0; \Omega))$ then, there exists a unique $\boldsymbol{\varphi} \in H(\mathbf{curl}; \Omega) \cap H(\text{div}_\epsilon^0; \Omega)$, such that $\gamma_t(\boldsymbol{\varphi}) = \mathbf{g}$. Moreover, by noting that $\mathbf{u} - \boldsymbol{\varphi} \in \mathbf{X}_{QP}$ is a solution of (3), we can conclude the uniqueness of \mathbf{u} ; from which the existence and uniqueness of the solution of (2) is deduced. \square

3 The HDG Method

Let us begin by setting a shape-regular simplicial tetrahedrization \mathcal{T}_h of Ω , such that each $\overset{\circ}{K} \in \mathcal{T}_h$ is completely contained in Ω_m or Ω_d . Then, \mathcal{T}_h^m and \mathcal{T}_h^d will denote the sets of tetrahedra lying in Ω_m and Ω_d , respectively. Furthermore, we define $\partial\mathcal{T}_h := \{\partial K : K \in \mathcal{T}_h\}$ and $\mathcal{E}_h := \mathcal{E}_I \cup \mathcal{E}_\Gamma$, where \mathcal{E}_I and \mathcal{E}_Γ denote the interior and boundary faces induced by \mathcal{T}_h , respectively. Due to the definition of Γ , we will denote by \mathcal{E}_0 and \mathcal{E}_{QP} the set of faces lying on Γ_0 and Γ_{QP} , respectively. We assume \mathcal{T}_h does not have hanging nodes. Moreover, let us also suppose conformity between the discretization of the periodic boundaries Γ_1 - Γ_2 and Γ_3 - Γ_4 . More precisely, if $F_1 = \{(0, y, z)\}$ is a face of Γ_1 , we assume that $F_2 := \{(L, y, z)\}$ is a face of Γ_2 . Similarly for Γ_3 and Γ_4 . In addition, we set $\|\cdot\|_{\mathcal{T}_h} := (\cdot, \cdot)_{\mathcal{T}_h}^{1/2}$ and $\|\cdot\|_{\partial\mathcal{T}_h} := (\cdot, \cdot)_{\partial\mathcal{T}_h}^{1/2}$, with

$$(\cdot, \cdot)_{\mathcal{T}_h} := \sum_{K \in \mathcal{T}_h} (\cdot, \cdot)_K, \quad \langle \cdot, \cdot \rangle_{\partial\mathcal{T}_h} := \sum_{K \in \mathcal{T}_h} \langle \cdot, \cdot \rangle_{\partial K},$$

where $(\cdot, \cdot)_D$ and $\langle \cdot, \cdot \rangle_G$ denote standard L^2 -complex inner products over regions $D \subset \mathbb{R}^3$ and $G \subset \mathbb{R}^2$, respectively.

For a vector-valued function \mathbf{w} , we define the tangential jump across $F \in \mathcal{E}_I$ by $[\![\mathbf{w}]\!]_F := \mathbf{w}^+ \times \mathbf{n}^+ + \mathbf{w}^- \times \mathbf{n}^-$. If $F \in \mathcal{E}_0$, we set $[\![\mathbf{w}]\!]_F := \mathbf{w} \times \mathbf{n}$. We will drop the subscript F , when there is no confusion. Let us now explain the jump operator acting on a face of a quasi-periodic boundary. If $F \subset \Gamma_1$, we define $[\![\mathbf{w}]\!]_{QP} := (e^{i\alpha L} \mathbf{w} \times \mathbf{n})|_{\Gamma_1} + (\mathbf{w} \times \mathbf{n})|_{\Gamma_2}$. In other words, if \mathbf{w} is quasi-periodic on Γ_1 , then $[\![\mathbf{w}]\!]_{QP} = 0$. Similarly, if $F \subset \Gamma_3$, we define $[\![\mathbf{w}]\!]_{QP} := (e^{i\beta L} \mathbf{w} \times \mathbf{n})|_{\Gamma_3} + (\mathbf{w} \times \mathbf{n})|_{\Gamma_4}$. For a scalar-valued function p , the jump across a face $F \in \mathcal{E}_I$ is denoted by $[\![q]\!] := q^+ - q^-$, whereas for a boundary face $F \in \mathcal{E}_\Gamma$, we write $[\![q]\!] := q$.

Considering the above tetrahedrization of $\overline{\Omega}$, we define the following approximation spaces

$$\begin{aligned} Q_h &:= \{q \in L^2(\Omega) : q|_K \in \mathbb{P}_k(K), \forall K \in \mathcal{T}_h\}, \\ M_h &:= \{q \in L^2(\mathcal{E}_h) : q|_F \in \mathbb{P}_k(F), \forall F \in \mathcal{E}_h\}, \\ \mathbf{V}_h &:= \{\mathbf{w} \in \mathbf{L}^2(\Omega) : \mathbf{w}|_K \in \mathbf{P}_k(K), \forall K \in \mathcal{T}_h\}, \\ \mathbf{M}'_h &:= \{\boldsymbol{\rho} \in \mathbf{L}^2(\mathcal{E}_h) : \boldsymbol{\rho}|_F \in \mathbf{P}_k(F), (\boldsymbol{\rho} \cdot \mathbf{n})|_F = 0, \forall F \in \mathcal{E}_h\}, \\ \mathbf{M}^g_{QP} &:= \left\{ \boldsymbol{\rho} \in \mathbf{M}'_h : \boldsymbol{\rho}|_{\Gamma_2} = e^{i\alpha L} \boldsymbol{\rho}|_{\Gamma_1}, \boldsymbol{\rho}|_{\Gamma_4} = e^{i\beta L} \boldsymbol{\rho}|_{\Gamma_3}, \boldsymbol{\rho}|_{\Gamma_0} \times \mathbf{n} = \mathbf{P}_{\mathbf{M}'_h} \mathbf{g} \right\} \end{aligned}$$

where $\mathbf{P}_{\mathbf{M}'_h}$ is L^2 -projections over \mathbf{M}'_h .

The HDG scheme associated to (2) seeks the approximation $(\mathbf{v}_h, \mathbf{u}_h, p_h, \widehat{\mathbf{u}}_h^t, \widehat{p}_h) \in \mathbf{V}_h \times \mathbf{V}_h \times Q_h \times \mathbf{M}^g_{QP} \times M_h$ of the exact solution $(\mathbf{v}, \mathbf{u}, p, \mathbf{u}^t|_{\mathcal{E}_h}, p|_{\mathcal{E}_h})$, satisfying

$$(\mathbf{v}_h, \mathbf{w})_{\mathcal{T}_h} - (\mathbf{u}_h, \nabla \times \mathbf{w})_{\mathcal{T}_h} - \langle \widehat{\mathbf{u}}_h^t, \mathbf{w} \times \mathbf{n} \rangle_{\partial\mathcal{T}_h} = 0, \tag{4a}$$

$$\begin{aligned} (\mathbf{v}_h, \nabla \times \mathbf{z})_{\mathcal{T}_h} + \langle \widehat{\mathbf{v}}_h^t, \mathbf{z} \times \mathbf{n} \rangle_{\partial\mathcal{T}_h} - \kappa^2 (\boldsymbol{\epsilon} \mathbf{u}_h, \mathbf{z})_{\mathcal{T}_h} - (p_h, \nabla \cdot (\boldsymbol{\epsilon} \mathbf{z}))_{\mathcal{T}_h} \\ + \langle \widehat{p}_h, \boldsymbol{\epsilon} \mathbf{z} \cdot \mathbf{n} \rangle_{\partial\mathcal{T}_h} = (\mathbf{f}, \mathbf{z})_{\mathcal{T}_h}, \end{aligned} \tag{4b}$$

$$- (\boldsymbol{\epsilon} \mathbf{u}_h, \nabla q)_{\mathcal{T}_h} + \langle \boldsymbol{\epsilon} \mathbf{u}_h^n \cdot \mathbf{n}, q \rangle_{\partial\mathcal{T}_h} = 0, \tag{4c}$$

$$\langle \mathbf{n} \times \widehat{\mathbf{v}}_h^t, \boldsymbol{\rho} \rangle_{\partial\mathcal{T}_h} = 0, \tag{4d}$$

$$\langle \widehat{\boldsymbol{\epsilon} \mathbf{u}_h^n \cdot \mathbf{n}}, \varrho \rangle_{\partial\mathcal{T}_h \setminus \Gamma} = 0, \tag{4e}$$

$$\langle \widehat{p}_h, \varrho \rangle_\Gamma = 0, \tag{4f}$$

for all $(\mathbf{w}, \mathbf{z}, q, \boldsymbol{\rho}, \varrho) \in \mathbf{V}_h \times \mathbf{V}_h \times Q_h \times \mathbf{M}_{\text{QP}}^0 \times M_h$, where the *numerical fluxes* $\widehat{\mathbf{v}}_h^t$ and $\widehat{\mathbf{u}}_h^n$ defined on ∂T_h are given by

$$\mathbf{n} \times \widehat{\mathbf{v}}_h^t := \mathbf{n} \times \mathbf{v}_h^t + \tau(\mathbf{u}_h^t - \widehat{\mathbf{u}}_h^t), \tag{4g}$$

$$\widehat{\mathbf{u}}_h^n \cdot \mathbf{n} := \epsilon \mathbf{u}_h^n \cdot \mathbf{n} + \tau_n(p_h - \widehat{p}_h). \tag{4h}$$

The stabilization parameters τ and τ_n are complex-valued that satisfy $\text{Re}(\tau) \geq 0, \text{Im}(\tau) \leq 0, \text{Re}(\tau_n) \geq 0$ and $\text{Im}(\tau_n) \geq 0$. These conditions ensure well-posedness of the scheme in agreement with Section 3 of [10].

We notice that, since the test function $\boldsymbol{\rho}$ belongs to \mathbf{M}_{QP}^0 , (4d) implies the quasi-periodicity of the numerical flux $\widehat{\mathbf{v}}_h^t$. In fact, taking $\boldsymbol{\rho} \neq 0$ on $\Gamma_1 \cup \Gamma_2$ and $\boldsymbol{\rho} = 0$ otherwise, we have that

$$\langle \mathbf{n} \times \widehat{\mathbf{v}}_h^t, \boldsymbol{\rho} \rangle_{\Gamma_1} + \langle \mathbf{n} \times \widehat{\mathbf{v}}_h^t, \boldsymbol{\rho} \rangle_{\Gamma_2} = 0,$$

for all $\boldsymbol{\rho} \in \mathbf{P}_k(\Gamma_1)$, due to the fact that $\boldsymbol{\rho}|_{\Gamma_2} = e^{i\alpha L} \boldsymbol{\rho}|_{\Gamma_1}$. Now, if we denote by φ the bijective mapping that transforms a face in Γ_2 into its corresponding face in Γ_1 , it holds

$$0 = \langle \mathbf{n} \times \widehat{\mathbf{v}}_h^t, \boldsymbol{\rho} \rangle_{\Gamma_1} + \langle (\mathbf{n} \times \widehat{\mathbf{v}}_h^t) \circ \varphi, e^{i\alpha L} \boldsymbol{\rho} \rangle_{\Gamma_1} = \langle \mathbf{n} \times \widehat{\mathbf{v}}_h^t + (\mathbf{n} \times \widehat{\mathbf{v}}_h^t) \circ \varphi e^{-i\alpha L}, \boldsymbol{\rho} \rangle_{\Gamma_1},$$

for all $\boldsymbol{\rho} \in \mathbf{P}_k(\Gamma_1)$, from which,

$$0 = (\mathbf{n} \times \widehat{\mathbf{v}}_h^t + (\mathbf{n} \times \widehat{\mathbf{v}}_h^t) \circ \varphi e^{-i\alpha L})|_{\Gamma_1} = \mathbf{n} \times \widehat{\mathbf{v}}_h^t|_{\Gamma_1} + \mathbf{n} \times \widehat{\mathbf{v}}_h^t e^{-i\alpha L}|_{\Gamma_2}.$$

Remark 1 We emphasize that $\widehat{\mathbf{u}}_h^t$ and $\widehat{\mathbf{v}}_h^t$ are “single-valued” on any face $F \in \mathcal{E}_h \setminus \mathcal{E}_{\text{QP}}$. Moreover, for faces in \mathcal{E}_{QP} , the numerical fluxes are also single-valued, but in a “quasi-periodic sense”, namely, $[[\widehat{\mathbf{u}}_h^t]]_{\text{QP}} = 0$ and $[[\widehat{\mathbf{v}}_h^t]]_{\text{QP}} = 0$.

The authors in [10] analyzed the well-posedness and provided the error estimates for an HDG scheme similar to (4), but considered a prescribed boundary data \mathbf{g} in the entire boundary Γ . In our case, quasi-periodic boundary conditions are imposed on the vertical walls. This quasi-periodicity is imposed strongly on the space \mathbf{M}_{QP}^g for the numerical trace $\widehat{\mathbf{u}}_h^t$ and implies the quasi-periodicity of the flux $\widehat{\mathbf{v}}_h^t$, as it was explained before. These facts make possible to cancel out the contribution of the terms on Γ_1 and Γ_2 (Γ_3 and Γ_4), during the deduction of the stability estimates of the scheme. Therefore, the same error analysis performed in [10] holds for (4). Even more, the analysis in it implies the following result for $s \in (0, 1)$ and $s \leq t$ chosen as in section 3.2 of the same reference.

Corollary 1 Let $(\mathbf{v}, \mathbf{u}, p) \in \mathbf{H}^{l_v+1}(\mathcal{T}_h) \times \mathbf{H}^{l_u+1}(\mathcal{T}_h) \times H^{l_p+1}(\mathcal{T}_h)$ and $(\mathbf{v}_h, \mathbf{u}_h, p_h, \widehat{\mathbf{u}}_h^t, \widehat{p}_h) \in \mathbf{V}_h \times \mathbf{V}_h \times Q_h \times \mathbf{M}_{\text{QP}}^g \times M_h$ be the solutions of (2) and (4), respectively, for $l_v, l_u, l_p \in [0, k]$. If τ and τ_n are purely imaginary, $s \in (0, 1)$ and $s \leq t$, there hold

$$\begin{aligned} \|\mathbf{v} - \mathbf{v}_h\|_{\mathcal{T}_h} &\lesssim h^{\min\{s, 1/2\}} \left(h^{l_v} |\mathbf{v}|_{l_v+1, \mathcal{T}_h} + h^{l_u} |\mathbf{u}|_{l_u+1, \mathcal{T}_h} + h^{l_p} |p|_{l_p+1, \mathcal{T}_h} \right) \\ \|\epsilon(\mathbf{u} - \mathbf{u}_h)\|_{\mathcal{T}_h} &\lesssim h^s \left(h^{l_v} |\mathbf{v}|_{l_v+1, \mathcal{T}_h} + h^{l_u} |\mathbf{u}|_{l_u+1, \mathcal{T}_h} + h^{l_p} |p|_{l_p+1, \mathcal{T}_h} \right), \end{aligned}$$

when $|\tau|$ and $|\tau_n|$ are of order one. If $|\tau|$ is of order h^{-1} and $|\tau_n|$ is of order h , then

$$\begin{aligned} \|\mathbf{v} - \mathbf{v}_h\|_{\mathcal{T}_h} &\lesssim h^{l_v + \min\{1, t\}} |\mathbf{v}|_{l_v+1, \mathcal{T}_h} + h^{l_u + \min\{0, t-1\}} |\mathbf{u}|_{l_u+1, \mathcal{T}_h} + h^{l_p + \min\{s+1, t\}} |p|_{l_p+1, \mathcal{T}_h} \\ \|\epsilon(\mathbf{u} - \mathbf{u}_h)\|_{\mathcal{T}_h} &\lesssim h^{l_v + \min\{1, t\}} |\mathbf{v}|_{l_v+1, \mathcal{T}_h} + h^{l_u + \min\{s, t-1\}} |\mathbf{u}|_{l_u+1, \mathcal{T}_h} + h^{l_p + 1 + \min\{s, t-1\}} |p|_{l_p+1, \mathcal{T}_h}. \end{aligned}$$

In addition, if τ and τ_n are not purely imaginary, then there exists $h_0 > 0$ such that for all $h < h_0$, the same result holds.

Remark 2 The numerical experiments reported in [10] show an experimental order of convergence better than the one predicted by the theory. More precisely, for smooth solutions and stabilization parameters with modulus proportional to one, the experimental rate of convergence is h^{k+1} for the L^2 -error of the approximations of \mathbf{u} , \mathbf{v} and p .

4 A Posteriori error analysis

In this section assuming that $|\tau|$ and $|\tau_n|$ with modulus proportional to one, we propose ‘under some circumstances’ a reliable and locally efficient error estimator for the energy-type error

$$\begin{aligned}
 E_h := & \|\mathbf{v} - \mathbf{v}_h\|_{\mathcal{T}_h} + \|\nabla \times (\mathbf{u} - \mathbf{u}_h)\|_{\mathcal{T}_h} + h^{-1/2} \\
 & \|\tau^{1/2}(\mathbf{u}_h^t - \widehat{\mathbf{u}}_h^t)\|_{\partial\mathcal{T}_h} \\
 & + h^{-1/2}\|\tau_n^{1/2}(p_h - \widehat{p}_h)\|_{\partial\mathcal{T}_h} + \|\nabla(p - p_h)\|_{\mathcal{T}_h} + \|\mathbf{u} - \mathbf{u}_h\|_{\mathcal{T}_h} + \|p - p_h\|_{\mathcal{T}_h}.
 \end{aligned}
 \tag{5}$$

According to Remark 2, the order of convergence of E_h is h^k when the solution is sufficiently smooth.

We base our analysis on the techniques presented in [13], but keeping in mind that, in our context Ω is occupied by an heterogeneous material because the relative permittivity is a complex-valued function.

Let us begin by defining the global error indicator:

$$\eta := \sum_{K \in \mathcal{T}_h} \left(\eta_K^2 + \sum_{F \subset \partial K} \eta_{F,1}^2 + \eta_{F,2}^2 + \eta_{F,3}^2 \right) + \sum_{F \in \mathcal{E}_I} \eta_{F,4}^2,$$

where η_K , $\eta_{F,1}$, $\eta_{F,2}$, $\eta_{F,3}$ and $\eta_{F,4}$ correspond to the local *a posteriori* error indicators, specified as follows.

For each $K \in \mathcal{T}_h$,

$$\eta_{K,1} := h_K \|\mathbf{f} - \bar{\epsilon} \nabla p_h + \kappa^2 \epsilon \mathbf{u}_h - \nabla \times (\nabla \times \mathbf{u}_h)\|_K,
 \tag{6a}$$

$$\eta_{K,2} := h_K \|\nabla \cdot \mathbf{f} + \kappa^2 \epsilon \nabla \cdot \mathbf{u}_h - \nabla \cdot (\bar{\epsilon} \nabla p_h)\|_K,
 \tag{6b}$$

and for $F \subset \partial K$,

$$\eta_{F,1} := h_F^{-1/2} \|\tau^{1/2}(\mathbf{u}_h - \widehat{\mathbf{u}}_h^t) \times \mathbf{n}\|_F,
 \tag{6c}$$

$$\eta_{F,2} := h_F^{-1/2} \|\tau_n^{1/2}(p_h - \widehat{p}_h)\|_F,
 \tag{6d}$$

$$\eta_{F,3} := h_F^{1/2} \|(\mathbf{v}_h - \nabla \times \mathbf{u}_h) \times \mathbf{n}\|_F.
 \tag{6e}$$

Moreover, for each $F \in \mathcal{E}_I$,

$$\eta_{F,4} := h_F^{1/2} \left\| \left[\left[\bar{\epsilon} \frac{\partial p_h}{\partial \mathbf{n}} \right] \right] \right\|_F.
 \tag{6f}$$

In order to state the main result, we denote by Π_V and Π_Q the L^2 -projections over \mathbf{V}_h and Q_h , see [18].

Theorem 1 *Let $(\mathbf{v}, \mathbf{u}, p) \in H(\mathbf{curl}; \Omega) \times \mathbf{X}_{\text{QP}}^{\mathbf{g}} \times H_0^1(\Omega)$ and $(\mathbf{v}_h, \mathbf{u}_h, p_h, \widehat{\mathbf{u}}_h^t, \widehat{p}_h) \in \mathbf{V}_h \times \mathbf{V}_h \times Q_h \times \mathbf{M}_{\text{QP}}^{\mathbf{g}} \times M_h$ be the solutions of (2) and (4), respectively. Then, there exist $C_1, C_2 > 0$ such that*

$$E_h \leq C_1 \eta \quad \wedge \quad C_2 \eta \leq E_h + \text{osc}_{\mathbf{f}} + \text{osc}_{\nabla \cdot \mathbf{f}},$$

where $\text{osc}_{\mathbf{f}} := \sum_{K \in \mathcal{T}_h} \text{osc}(\mathbf{f}, K)$, $\text{osc}(\mathbf{f}, K) := h_K \|\mathbf{f} - \Pi_{\mathbf{V}} \mathbf{f}\|_K$, $\text{osc}_{\nabla \cdot \mathbf{f}} := \sum_{K \in \mathcal{T}_h} \text{osc}(\nabla \cdot \mathbf{f}, K)$ and $\text{osc}(\nabla \cdot \mathbf{f}, K) := h_K \|\nabla \cdot \mathbf{f} - \Pi_Q(\nabla \cdot \mathbf{f})\|_K$.

In the forthcoming sections we will derive a sequence of results that will lead to the proof of Theorem 1. We will employ approximation properties for discontinuous functions and bubble functions.

4.1 Reliability

One of the main tools, usually employed in the context of DG methods is the conforming approximation of a piecewise polynomial function. In this direction, we obtained the following lemmas by using Proposition 4.5 of [25] and Theorem 2.2 of [29].

Lemma 2 *Let $\mathbf{w} \in \mathbf{V}_h$ and $\widetilde{\mathbf{g}}$ be the tangential trace of a function in $\mathbf{V}_h^c := \mathbf{V}_h \cap H(\mathbf{curl}; \Omega)$. Then, there exists $\mathbf{w}^c \in \mathbf{V}_h^c$ with $\mathbf{w}^c \times \mathbf{n}|_{\Gamma_0} = \widetilde{\mathbf{g}}$, such that*

$$\|\mathbf{w} - \mathbf{w}^c\|_{\mathcal{T}_h} \lesssim \|h^{1/2} \llbracket \mathbf{w} \rrbracket\|_{\mathcal{E}_h \setminus \mathcal{E}_0} + \|h^{1/2}(\mathbf{w} \times \mathbf{n} - \widetilde{\mathbf{g}})\|_{\mathcal{E}_0}, \tag{7a}$$

$$\|\nabla \times (\mathbf{w} - \mathbf{w}^c)\|_{\mathcal{T}_h} \lesssim \|h^{-1/2} \llbracket \mathbf{w} \rrbracket\|_{\mathcal{E}_h \setminus \mathcal{E}_0} + \|h^{-1/2}(\mathbf{w} \times \mathbf{n} - \widetilde{\mathbf{g}})\|_{\mathcal{E}_0}. \tag{7b}$$

Moreover, there exists $\mathbf{w}^{\text{QP}} \in \mathbf{V}_h^c$ with tangential trace $\widetilde{\mathbf{g}}$ on Γ_0 and quasi-periodic conditions on Γ_{QP} , such that

$$\|\mathbf{w} - \mathbf{w}^{\text{QP}}\|_{\mathcal{T}_h} \lesssim \|h^{1/2} \llbracket \mathbf{w} \rrbracket\|_{\mathcal{E}_I} + \|h^{1/2} \llbracket \mathbf{w} \rrbracket_{\text{QP}}\|_{\mathcal{E}_{\text{QP}}} + \|h^{1/2}(\mathbf{w} \times \mathbf{n} - \widetilde{\mathbf{g}})\|_{\mathcal{E}_0}, \tag{7c}$$

$$\|\nabla \times (\mathbf{w} - \mathbf{w}^{\text{QP}})\|_{\mathcal{T}_h} \lesssim \|h^{-1/2} \llbracket \mathbf{w} \rrbracket\|_{\mathcal{E}_I} + \|h^{-1/2} \llbracket \mathbf{w} \rrbracket_{\text{QP}}\|_{\mathcal{E}_{\text{QP}}} + \|h^{-1/2}(\mathbf{w} \times \mathbf{n} - \widetilde{\mathbf{g}})\|_{\mathcal{E}_0}. \tag{7d}$$

In addition, let $q \in Q_h$. There exists $q^c \in Q_h^c := Q_h \cap H_0^1(\Omega)$, such that

$$\|\nabla(q - q^c)\|_{\mathcal{T}_h} \lesssim \|h^{-1/2} \llbracket q \rrbracket\|_{\mathcal{E}_I} \lesssim \|h^{-1/2}(q - \varrho)\|_{\partial \mathcal{T}_h}, \tag{7e}$$

for any singled-valued function ϱ defined over \mathcal{E}_h , such and $\varrho|_{\Gamma} = 0$.

The estimates (7a) and (7b) were proven in Proposition 4.5 of [25], whereas the proof of (7e) can be found in Theorem 2.2 of [29]. The results in (7c) and (7d) are consequence of (7a) and its proof will be postponed to the appendix (Appendix A.2).

In addition, we will employ the Scott-Zhang interpolant $\Pi_{\text{SZ}} : H_{\vartheta}^1(\Omega) \rightarrow Q_h \cap H_{\vartheta}^1(\Omega)$, where $H_{\vartheta}^1(\Omega) := \{\phi \in H^1(\Omega) : \phi|_{\vartheta} = 0\}$ with $\vartheta \subseteq \Gamma$. Note that if $\phi \in H_0^1(\Omega)$ then $\Pi_{\text{SZ}} \phi \in Q_h^c$. In the literature, it is known that it satisfies the following approximation properties [cf. [44]].

Lemma 3 *Let $K \in \mathcal{T}_h$ and $F \in \mathcal{E}_h$. For any $\phi \in H_{\vartheta}^1(\Omega)$, there hold*

$$\|\phi - \Pi_{\text{SZ}} \phi\|_K \lesssim h_K |\phi|_{1, \omega_K},$$

$$\|\phi - \Pi_{\text{SZ}} \phi\|_F \lesssim h_F^{1/2} |\phi|_{1, \omega_F},$$

where $\omega_K := \cup\{K' \in \mathcal{T}_h : \overline{K'} \cap \overline{K} \neq \emptyset\}$ and $\omega_F := \cup\{K' \in \mathcal{T}_h : \overline{K'} \cap \overline{F} \neq \emptyset\}$.

Now, we are in position to prove an upper bound for the L^2 and broken H^1 - error on the pressure. As we will see, this bound depends on some of the terms of the error estimator and also on the L^2 -error of the electric field. For the sake of simplicity in the exposition, from now on we assume that \mathbf{g} is the tangential trace of a function in \mathbf{V}_h^c . Otherwise, oscillatory terms related to \mathbf{g} would appear.

Lemma 4 For $(\mathbf{v}, \mathbf{u}, p) \in \mathbf{H}(\text{curl}; \Omega) \times \mathbf{X}_{\text{QP}}^{\mathbf{g}} \times H_0^1(\Omega)$ and $(\mathbf{v}_h, \mathbf{u}_h, p_h, \widehat{\mathbf{u}}_h^t, \widehat{p}_h) \in \mathbf{V}_h \times \mathbf{V}_h \times Q_h \times \mathbf{M}_{\text{QP}}^{\mathbf{g}} \times M_h$ the solutions of (2) and (4), respectively, there hold

$$\|p - p_h\|_{\mathcal{T}_h} \lesssim \|\nabla(p - p_h)\|_{\mathcal{T}_h} + \|h^{-1/2}(p_h - \widehat{p}_h)\|_{\partial\mathcal{T}_h}, \tag{8a}$$

$$\|\nabla(p - p_h)\|_{\mathcal{T}_h} \lesssim \sum_{K \in \mathcal{T}_h} \eta_{K,2} + \sum_{F \in \mathcal{E}_I} \eta_{F,4} + \kappa^2 \|\epsilon(\mathbf{u} - \mathbf{u}_h)\|_{\mathcal{T}_h} + \|h^{-1/2}(p_h - \widehat{p}_h)\|_{\partial\mathcal{T}_h}. \tag{8b}$$

Proof By the discrete Poincaré inequality ([18], Corollary 5.4) and the fact that \widehat{p}_h is single-valued and vanishes at the boundary, we have that

$$\begin{aligned} \|p - p_h\|_{\mathcal{T}_h} &\lesssim \|\nabla(p - p_h)\|_{\mathcal{T}_h} + \|h^{-1/2} \llbracket p_h \rrbracket\|_{\mathcal{E}_I} + \|h^{-1/2} p_h\|_{\mathcal{E}_\Gamma} \\ &\lesssim \|\nabla(p - p_h)\|_{\mathcal{T}_h} + \|h^{-1/2} \llbracket p_h - \widehat{p}_h \rrbracket\|_{\mathcal{E}_I} + \|h^{-1/2}(p_h - \widehat{p}_h)\|_{\mathcal{E}_\Gamma} \\ &\lesssim \|\nabla(p - p_h)\|_{\mathcal{T}_h} + \|h^{-1/2}(p_h - \widehat{p}_h)\|_{\partial\mathcal{T}_h}, \end{aligned}$$

from which (8a) follows. Now, in order to bound $\|\nabla(p - p_h)\|_{\mathcal{T}_h}$, we employ the result in Lemma 2. More precisely, for $p_h \in Q_h$ there exists $p_h^c \in Q_h^c$ such that

$$\|\nabla(p_h - p_h^c)\|_{\mathcal{T}_h} \lesssim \|h^{-1/2}(p_h - \widehat{p}_h)\|_{\partial\mathcal{T}_h}. \tag{9}$$

On the other hand, by substituting \mathbf{f} [cf. (2b)] in (4b) we obtain the next error equation

$$\begin{aligned} (\mathbf{v} - \mathbf{v}_h, \nabla \times \mathbf{z})_{\mathcal{T}_h} + \langle \mathbf{v}^t - \widehat{\mathbf{v}}_h^t, \mathbf{z} \times \mathbf{n} \rangle_{\partial\mathcal{T}_h} - \kappa^2 \langle \epsilon(\mathbf{u} - \mathbf{u}_h), \mathbf{z} \rangle_{\mathcal{T}_h} \\ + \langle \bar{\epsilon} \nabla(p - p_h), \mathbf{z} \rangle_{\mathcal{T}_h} + \langle p_h - \widehat{p}_h, \epsilon \mathbf{z} \cdot \mathbf{n} \rangle_{\partial\mathcal{T}_h} = 0 \\ \forall \mathbf{z} \in \mathbf{V}_h. \end{aligned} \tag{10}$$

Let $\phi := p - p_h^c \in H_0^1(\Omega)$, by taking $\mathbf{z} := \nabla \Pi_{\text{SZ}} \phi$ in (10), it follows that

$$-\kappa^2 \langle \epsilon(\mathbf{u} - \mathbf{u}_h), \nabla \Pi_{\text{SZ}} \phi \rangle_{\mathcal{T}_h} + \langle \bar{\epsilon} \nabla(p - p_h), \nabla \Pi_{\text{SZ}} \phi \rangle_{\mathcal{T}_h} + \langle p_h - \widehat{p}_h, \epsilon \nabla \Pi_{\text{SZ}} \phi \cdot \mathbf{n} \rangle_{\partial\mathcal{T}_h} = 0,$$

since $\nabla \times \nabla \Pi_{\text{SZ}} \phi = 0$ and $\langle \mathbf{v}^t - \widehat{\mathbf{v}}_h^t, \nabla \Pi_{\text{SZ}} \phi \times \mathbf{n} \rangle_{\partial\mathcal{T}_h} = 0$. Then, if we rewrite $\langle \bar{\epsilon} \nabla(p - p_h), \epsilon \nabla \phi \rangle_{\mathcal{T}_h}$ by using the above expression and the Green’s identity of $\mathbf{H}(\text{div}_\epsilon; \mathcal{T}_h)$, we obtain that

$$\begin{aligned} \langle \nabla(p - p_h), \epsilon \nabla \phi \rangle_{\mathcal{T}_h} &= \langle \nabla(p - p_h), \epsilon \nabla(\phi - \Pi_{\text{SZ}} \phi) \rangle_{\mathcal{T}_h} \\ &\quad + \langle \nabla(p - p_h), \epsilon \nabla \Pi_{\text{SZ}} \phi \rangle_{\mathcal{T}_h} \\ &= \langle \nabla(p - p_h), \epsilon \nabla(\phi - \Pi_{\text{SZ}} \phi) \rangle_{\mathcal{T}_h} \\ &\quad + \kappa^2 \langle \epsilon(\mathbf{u} - \mathbf{u}_h), \nabla \Pi_{\text{SZ}} \phi \rangle_{\mathcal{T}_h} \\ &\quad - \langle p_h - \widehat{p}_h, \epsilon \nabla \Pi_{\text{SZ}} \phi \cdot \mathbf{n} \rangle_{\partial\mathcal{T}_h} \\ &= -\langle \nabla \cdot (\bar{\epsilon} \nabla(p - p_h)), \phi - \Pi_{\text{SZ}} \phi \rangle_{\mathcal{T}_h} \\ &\quad + \langle \bar{\epsilon} \nabla(p - p_h) \cdot \mathbf{n}, \phi - \Pi_{\text{SZ}} \phi \rangle_{\partial\mathcal{T}_h} \\ &\quad - \kappa^2 \langle \nabla \cdot (\epsilon(\mathbf{u} - \mathbf{u}_h)), \Pi_{\text{SZ}} \phi \rangle_{\mathcal{T}_h} \\ &\quad + \kappa^2 \langle \epsilon(\mathbf{u} - \mathbf{u}_h) \cdot \mathbf{n}, \Pi_{\text{SZ}} \phi \rangle_{\partial\mathcal{T}_h} \\ &\quad - \langle \bar{\epsilon} (p_h - \widehat{p}_h), \nabla \Pi_{\text{SZ}} \phi \cdot \mathbf{n} \rangle_{\partial\mathcal{T}_h}. \end{aligned}$$

Moreover, by Eq. (2b), we deduce that

$$\begin{aligned}
 (\nabla(p - p_h), \epsilon \nabla \phi)_{\mathcal{T}_h} &= (\nabla \cdot \mathbf{f} + \kappa^2 \nabla \cdot (\epsilon \mathbf{u}_h) - \nabla \cdot (\bar{\epsilon} \nabla p_h), \Pi_{\text{SZ}} \phi - \phi)_{\mathcal{T}_h} \\
 &\quad + (\bar{\epsilon} \nabla(p - p_h) \cdot \mathbf{n}, \phi - \Pi_{\text{SZ}} \phi)_{\partial \mathcal{T}_h} \\
 &\quad - \kappa^2 (\nabla \cdot \epsilon(\mathbf{u} - \mathbf{u}_h), \phi)_{\mathcal{T}_h} \\
 &\quad + \kappa^2 \langle \epsilon(\mathbf{u} - \mathbf{u}_h) \cdot \mathbf{n}, \Pi_{\text{SZ}} \phi - \phi \rangle_{\partial \mathcal{T}_h} \\
 &\quad + \kappa^2 \langle \epsilon(\mathbf{u} - \mathbf{u}_h) \cdot \mathbf{n}, \phi \rangle_{\partial \mathcal{T}_h} - \langle \bar{\epsilon}(p_h - \hat{p}_h), \nabla \Pi_{\text{SZ}} \phi \cdot \mathbf{n} \rangle_{\partial \mathcal{T}_h} \\
 &= (\nabla \cdot \mathbf{f} + \kappa^2 \nabla \cdot (\epsilon \mathbf{u}_h) - \nabla \cdot (\bar{\epsilon} \nabla p_h), \Pi_{\text{SZ}} \phi - \phi)_{\mathcal{T}_h} \\
 &\quad + (\bar{\epsilon} \nabla(p - p_h) \cdot \mathbf{n}, \phi - \Pi_{\text{SZ}} \phi)_{\partial \mathcal{T}_h} + \kappa^2 (\epsilon(\mathbf{u} - \mathbf{u}_h), \nabla \phi)_{\mathcal{T}_h} \\
 &\quad + \kappa^2 \langle \epsilon(\mathbf{u} - \mathbf{u}_h) \cdot \mathbf{n}, \Pi_{\text{SZ}} \phi - \phi \rangle_{\partial \mathcal{T}_h} - \langle \bar{\epsilon}(p_h - \hat{p}_h), \\
 &\quad \nabla \Pi_{\text{SZ}} \phi \cdot \mathbf{n} - \nabla \Pi_{\text{Q}}^0 \phi \cdot \mathbf{n} \rangle_{\partial \mathcal{T}_h}, \tag{11}
 \end{aligned}$$

where Π_{Q}^0 is the L^2 -projection over $\mathbb{P}_0(\mathcal{T}_h)$.

Now, let us bound each term on the right hand side of (11). We apply the Cauchy-Schwarz inequality, the approximation properties in Lemma 3, inverse inequality and the continuity of $\bar{\epsilon} \nabla p \cdot \mathbf{n}$, which is derived from the second equation of (2) and the fact that $\mathbf{f} \in \mathbf{H}(\text{div}^0; \Omega)$. More precisely, for the first term, it holds

$$\begin{aligned}
 (\nabla \cdot \mathbf{f} + \kappa^2 \nabla \cdot (\epsilon \mathbf{u}_h) - \nabla \cdot (\bar{\epsilon} \nabla p_h), \Pi_{\text{SZ}} \phi - \phi)_{\mathcal{T}_h} \\
 \lesssim h \|\nabla \cdot \mathbf{f} + \kappa^2 \nabla \cdot (\epsilon \mathbf{u}_h) - \nabla \cdot (\bar{\epsilon} \nabla p_h)\|_{\mathcal{T}_h} \|\phi\|_{1, \mathcal{T}_h}
 \end{aligned}$$

and for the second term,

$$\begin{aligned}
 (\bar{\epsilon} \nabla(p - p_h) \cdot \mathbf{n}, \phi - \Pi_{\text{SZ}} \phi)_{\partial \mathcal{T}_h} &\lesssim h^{1/2} \|\bar{\epsilon} \nabla(p - p_h) \cdot \mathbf{n}\|_{\partial \mathcal{T}_h} \|\phi\|_{1, \mathcal{T}_h} \\
 &\lesssim \|h^{1/2} [\bar{\epsilon} \nabla p_h \cdot \mathbf{n}]\|_{\mathcal{E}_I} \|\phi\|_{1, \mathcal{T}_h}.
 \end{aligned}$$

Similarly, we derive the following bounds for the third, fourth and fifth terms

$$\begin{aligned}
 \kappa^2 (\epsilon(\mathbf{u} - \mathbf{u}_h), \nabla \phi)_{\mathcal{T}_h} &\lesssim \kappa^2 \|\epsilon(\mathbf{u} - \mathbf{u}_h)\|_{\mathcal{T}_h} \|\phi\|_{1, \mathcal{T}_h}, \\
 \kappa^2 \langle \epsilon(\mathbf{u} - \mathbf{u}_h) \cdot \mathbf{n}, \Pi_{\text{SZ}} \phi - \phi \rangle_{\partial \mathcal{T}_h} &\lesssim \kappa^2 \|\epsilon(\mathbf{u} - \mathbf{u}_h)\|_{\mathcal{T}_h} \|\phi\|_{1, \mathcal{T}_h}, \\
 \langle \bar{\epsilon}(p_h - \hat{p}_h), (\nabla \Pi_{\text{SZ}} \phi - \nabla \Pi_{\text{Q}}^0 \phi) \cdot \mathbf{n} \rangle_{\partial \mathcal{T}_h} &\lesssim \sum_{K \in \mathcal{T}_h} \|\bar{\epsilon}(p_h - \hat{p}_h)\|_{\partial K} \|(\nabla \Pi_{\text{SZ}} \phi - \nabla \Pi_{\text{Q}}^0 \phi) \cdot \mathbf{n}\|_{\partial K} \\
 &\lesssim \sum_{K \in \mathcal{T}_h} \|\bar{\epsilon}(p_h - \hat{p}_h)\|_{\partial K} h_K^{-1/2} \|\nabla \Pi_{\text{SZ}} \phi - \nabla \Pi_{\text{Q}}^0 \phi\|_K \\
 &\lesssim \sum_{K \in \mathcal{T}_h} h_K^{-3/2} \|\bar{\epsilon}(p_h - \hat{p}_h)\|_{\partial K} \|\Pi_{\text{SZ}} \phi - \Pi_{\text{Q}}^0 \phi\|_K \\
 &\lesssim \|h^{-1/2} \bar{\epsilon}(p_h - \hat{p}_h)\|_{\partial \mathcal{T}_h} \|\phi\|_{1, \mathcal{T}_h}.
 \end{aligned}$$

By replacing all the above bounds in (11), noticing that

$$\|\nabla(p - p_h^c)\|_{\mathcal{T}_h}^2 \lesssim |(\nabla(p - p_h), \epsilon \nabla \phi)_{\mathcal{T}_h}| + |(\nabla(p_h - p_h^c), \nabla \phi)_{\mathcal{T}_h}|,$$

considering Lemma 3 and using Poincaré inequality applied to $\|\phi\|_{\mathcal{T}_h}$, we deduce that

$$\begin{aligned}
 \|\nabla(p - p_h^c)\|_{\mathcal{T}_h} &\lesssim h \|\nabla \cdot \mathbf{f} + \kappa^2 \nabla \cdot (\epsilon \mathbf{u}_h) - \nabla \cdot (\bar{\epsilon} \nabla p_h)\|_{\mathcal{T}_h} + \|h^{1/2} [\bar{\epsilon} \nabla p_h \cdot \mathbf{n}]\|_{\mathcal{E}_I} \\
 &\quad + \kappa^2 \|\epsilon(\mathbf{u} - \mathbf{u}_h)\|_{\mathcal{T}_h} + \|h^{-1/2}(p_h - \hat{p}_h)\|_{\partial \mathcal{T}_h} + \|\nabla(p_h - p_h^c)\|_{\mathcal{T}_h}.
 \end{aligned}$$

Finally, writing $\nabla(p - p_h) = \nabla(p - p_h^c) + \nabla(p_h^c - p_h)$, using triangle inequality, (9) and the last expression, we obtain (8b). \square

In the next result, it is presented an upper bound for the L^2 -error of the electric field that depends on the L^2 -error of an approximation of its curl and the penalty terms. The former will be bounded later, by a computable quantity.

Lemma 5 *Let $(\mathbf{v}, \mathbf{u}, p) \in H(\mathbf{curl}; \Omega) \times \mathbf{X}_{QP}^{\mathbf{g}} \times H_0^1(\Omega)$ and $(\mathbf{v}_h, \mathbf{u}_h, p_h, \widehat{\mathbf{u}}_h^t, \widehat{p}_h) \in \mathbf{V}_h \times \mathbf{V}_h \times Q_h \times \mathbf{M}_{QP}^{\mathbf{g}} \times M_h$ be the solutions of (2) and (4), respectively. There holds*

$$\|\epsilon(\mathbf{u} - \mathbf{u}_h)\|_{\mathcal{T}_h} \lesssim \|\nabla \times (\mathbf{u} - \mathbf{u}_h^{QP})\|_{\mathcal{T}_h} + h^{1/2} \|\tau_n(p_h - \widehat{p}_h)\|_{\partial\mathcal{T}_h} + \|h^{1/2}(\mathbf{u}_h - \widehat{\mathbf{u}}_h^t) \times \mathbf{n}\|_{\partial\mathcal{T}_h} \tag{12}$$

where \mathbf{u}_h^{QP} is given by Lemma 2 for $\mathbf{u}_h \in \mathbf{V}_h$.

Proof First of all, thanks to Lemma 2, for $\mathbf{u}_h \in \mathbf{V}_h$ there exists $\mathbf{u}_h^{QP} \in \mathbf{V}_h^c$ with $\mathbf{u}_h^{QP} \times \mathbf{n} |_{\Gamma_0} = \mathbf{g}$ such that

$$\|\mathbf{u}_h - \mathbf{u}_h^{QP}\|_{\mathcal{T}_h} \lesssim \|h^{1/2} \llbracket \mathbf{u}_h \rrbracket\|_{\mathcal{E}_I} + \|h^{1/2} \llbracket \mathbf{u}_h \rrbracket_{QP}\|_{\mathcal{E}_{QP}} + \|h^{1/2}(\mathbf{u}_h \times \mathbf{n} - \mathbf{g})\|_{\mathcal{E}_0},$$

Even more, the facts that $\llbracket \widehat{\mathbf{u}}_h^t \rrbracket = \mathbf{0}$ on \mathcal{E}_I , $\llbracket \widehat{\mathbf{u}}_h^t \rrbracket_{QP} = \mathbf{0}$ on Γ_{QP} (cf. Remark 1) and $\widehat{\mathbf{u}}_h^t \times \mathbf{n} |_{\Gamma_0} = \mathbf{g}$, imply that

$$\|\mathbf{u}_h - \mathbf{u}_h^{QP}\|_{\mathcal{T}_h} \lesssim \|h^{1/2} \llbracket \mathbf{u}_h - \widehat{\mathbf{u}}_h^t \rrbracket\|_{\mathcal{E}_I} + \|h^{1/2} \llbracket \mathbf{u}_h - \widehat{\mathbf{u}}_h^t \rrbracket_{QP}\|_{\mathcal{E}_{QP}} + \|h^{1/2}(\mathbf{u}_h - \widehat{\mathbf{u}}_h^t) \times \mathbf{n}\|_{\mathcal{E}_0},$$

therefore, since ϵ is a bounded function, we have that

$$\|\epsilon(\mathbf{u}_h - \mathbf{u}_h^{QP})\|_{\mathcal{T}_h} \lesssim \|h^{1/2}(\mathbf{u}_h - \widehat{\mathbf{u}}_h^t) \times \mathbf{n}\|_{\partial\mathcal{T}_h}. \tag{13}$$

and, by the triangle inequality

$$\|\epsilon(\mathbf{u} - \mathbf{u}_h)\|_{\mathcal{T}_h} \lesssim \|\epsilon(\mathbf{u} - \mathbf{u}_h^{QP})\|_{\mathcal{T}_h} + \|h^{1/2}(\mathbf{u}_h - \widehat{\mathbf{u}}_h^t) \times \mathbf{n}\|_{\partial\mathcal{T}_h}. \tag{14}$$

Now, let us see the deduction of a bound for the term $\|\epsilon(\mathbf{u} - \mathbf{u}_h^{QP})\|_{\mathcal{T}_h}$. For this purpose, we will use a Helmholtz decomposition, which will be demonstrated in the Appendix A.1. For $\mathbf{u} - \mathbf{u}_h^{QP} \in \mathbf{L}^2(\Omega)$ there exist $\psi \in H_{\Gamma_0}^{1,QP}(\Omega)$ and $\mathbf{u}_s \in H_{\Gamma_{QP}}(\text{div}^0; \Omega)$, such that

$$\mathbf{u} - \mathbf{u}_h^{QP} = \nabla\psi + \mathbf{u}_s \tag{15}$$

and $\|\mathbf{u} - \mathbf{u}_h^{QP}\|_{\Omega}^2 = \|\nabla\psi\|_{\Omega}^2 + \|\mathbf{u}_s\|_{\Omega}^2$ (see Proposition 1). Moreover, according with [21, Theorem 8.4], since Ω is simply connected and $\mathbf{u}_s \in H_{\Gamma_{QP}}(\text{div}^0; \Omega)$ there exists a unique $\tilde{\mathbf{z}} \in H_{\Gamma_0}(\text{div}^0; \Omega) \cap H_{\Gamma_{QP}}(\mathbf{curl}; \Omega)$ such that $\nabla \times \tilde{\mathbf{z}} = \mathbf{u}_s$, and it satisfies

$$\|\tilde{\mathbf{z}}\|_{H(\mathbf{curl}; \Omega)} \lesssim \|\mathbf{u}_s\|_{\Omega}. \tag{16}$$

In the next part of the proof, we bound $\|\mathbf{u}_s\|_{\Omega}$ and $\|\nabla\psi\|_{\Omega}$. First, we note that $(\mathbf{u} - \mathbf{u}_h^{QP}) \times \mathbf{n} |_{\Gamma_0} = \mathbf{0}$, since $\mathbf{u} \in \mathbf{X}_{QP}^{\mathbf{g}}$ and \mathbf{g} is the tangential trace of \mathbf{u}_h^{QP} . By considering the orthogonal decomposition (15) and integrating by parts, we note that

$$\begin{aligned} \|\mathbf{u}_s\|_{\Omega}^2 &= (\mathbf{u}_s, \mathbf{u} - \mathbf{u}_h^{QP} - \nabla\psi)_{\Omega} = (\nabla \times \tilde{\mathbf{z}}, \mathbf{u} - \mathbf{u}_h^{QP})_{\Omega} - (\mathbf{u}_s, \nabla\psi)_{\Omega} \\ &= (\tilde{\mathbf{z}}, \nabla \times (\mathbf{u} - \mathbf{u}_h^{QP}))_{\Omega} + \langle (\mathbf{u} - \mathbf{u}_h^{QP}) \times \mathbf{n}, \tilde{\mathbf{z}} \rangle_{\Gamma} \\ &\quad + (\nabla \cdot \mathbf{u}_s, \psi)_{\Omega} - \langle \mathbf{u}_s \cdot \mathbf{n}, \psi \rangle_{\Gamma} = (\tilde{\mathbf{z}}, \nabla \times (\mathbf{u} - \mathbf{u}_h^{QP}))_{\Omega} \end{aligned}$$

where the first boundary term vanishes due to the fact that $\mathbf{u} - \mathbf{u}_h^{\text{QP}} \in H_{\Gamma_0}(\mathbf{curl}; \Omega)$, $\tilde{\mathbf{z}} \in H_{\Gamma_{\text{QP}}}(\mathbf{curl}; \Omega)$ and the other terms because $\mathbf{u}_s \in H_{\Gamma_{\text{QP}}}(\text{div}^0; \Omega)$ and $\psi|_{\Gamma_0} = 0$. Therefore, by the Cauchy-Schwarz inequality and (16), it holds

$$\|\mathbf{u}_s\|_{\Omega}^2 \lesssim \|\mathbf{u}_s\|_{\Omega} \|\nabla \times (\mathbf{u} - \mathbf{u}_h^{\text{QP}})\|_{\Omega},$$

thus

$$\|\mathbf{u}_s\|_{\Omega} \lesssim \|\nabla \times (\mathbf{u} - \mathbf{u}_h^{\text{QP}})\|_{\mathcal{T}_h}. \tag{17}$$

Now, in order to bound $\|\nabla \psi\|_{\Omega}$, we also employ the aforementioned orthogonal decomposition and the addition and subtraction of \mathbf{u}_h , as follows

$$\|\nabla \psi\|_{\Omega}^2 = (\mathbf{u} - \mathbf{u}_h^{\text{QP}} - \mathbf{u}_s, \nabla \psi)_{\Omega} = (\mathbf{u} - \mathbf{u}_h^{\text{QP}}, \nabla \psi)_{\Omega} = (\epsilon^{-1} \epsilon (\mathbf{u} - \mathbf{u}_h + \mathbf{u}_h - \mathbf{u}_h^{\text{QP}}), \nabla \psi)_{\mathcal{T}_h},$$

in order to conclude that,

$$\|\nabla \psi\|_{\Omega}^2 \lesssim |(\epsilon(\mathbf{u} - \mathbf{u}_h), \nabla \psi)_{\mathcal{T}_h}| + |(\epsilon(\mathbf{u}_h - \mathbf{u}_h^{\text{QP}}), \nabla \psi)_{\mathcal{T}_h}|. \tag{18}$$

Then, taking into account (2c) and (4c), we deduce the following error equation

$$-(\epsilon(\mathbf{u} - \mathbf{u}_h), \nabla q)_{\mathcal{T}_h} + \langle (\epsilon \mathbf{u} - \widehat{\epsilon \mathbf{u}_h^n}) \cdot \mathbf{n}, q \rangle_{\partial \mathcal{T}_h} = 0,$$

for all $q \in Q_h$. From which, after applying the Green’s identity of $H(\text{div}; \mathcal{T}_h)$, it is obtained that

$$(\nabla \cdot \epsilon(\mathbf{u} - \mathbf{u}_h), q)_{\mathcal{T}_h} + \langle (\epsilon \mathbf{u}_h - \widehat{\epsilon \mathbf{u}_h^n}) \cdot \mathbf{n}, q \rangle_{\partial \mathcal{T}_h} = 0 \quad \forall q \in Q_h. \tag{19}$$

Now, if we integrate by parts in the first term of (18), add and subtract $(\nabla \cdot \epsilon(\mathbf{u} - \mathbf{u}_h), \Pi_{\text{SZ}} \psi)_{\mathcal{T}_h}$, integrate by parts $(\nabla \cdot \epsilon(\mathbf{u} - \mathbf{u}_h), \Pi_{\text{SZ}} \psi)_{\mathcal{T}_h}$, use the fact that $\mathbf{u} \in H(\text{div}_{\epsilon}^0; \Omega)$ and choose $q = \Pi_{\text{SZ}} \psi \in Q_h$ in (19), we can get that

$$\begin{aligned} (\epsilon(\mathbf{u} - \mathbf{u}_h), \nabla \psi)_{\mathcal{T}_h} &= -(\nabla \cdot \epsilon(\mathbf{u} - \mathbf{u}_h), \psi)_{\mathcal{T}_h} + \langle \epsilon(\mathbf{u} - \mathbf{u}_h) \cdot \mathbf{n}, \psi \rangle_{\partial \mathcal{T}_h} \\ &= (\nabla \cdot \epsilon(\mathbf{u} - \mathbf{u}_h), \Pi_{\text{SZ}} \psi - \psi)_{\mathcal{T}_h} \\ &\quad - (\nabla \cdot \epsilon(\mathbf{u} - \mathbf{u}_h), \Pi_{\text{SZ}} \psi)_{\mathcal{T}_h} + \langle \epsilon(\mathbf{u} - \mathbf{u}_h) \cdot \mathbf{n}, \psi \rangle_{\partial \mathcal{T}_h} \\ &= (\nabla \cdot \epsilon(\mathbf{u}_h), \psi - \Pi_{\text{SZ}} \psi)_{\mathcal{T}_h} + \langle (\epsilon \mathbf{u} - \widehat{\epsilon \mathbf{u}_h^n}) \cdot \mathbf{n}, \Pi_{\text{SZ}} \psi \rangle_{\mathcal{E}_{\text{QP}}} \\ &\quad + \langle \epsilon(\mathbf{u} - \mathbf{u}_h) \cdot \mathbf{n}, \psi - \Pi_{\text{SZ}} \psi \rangle_{\partial \mathcal{T}_h \setminus (\mathcal{E}_{\text{QP}} \cup \mathcal{E}_0)}, \end{aligned}$$

where in the last step we have made use of the fact that $\langle (\epsilon \mathbf{u} - \widehat{\epsilon \mathbf{u}_h^n}) \cdot \mathbf{n}, \Pi_{\text{SZ}} \psi \rangle_{\partial \mathcal{T}_h \setminus \mathcal{E}_{\text{QP}}} = 0$, due to $\Pi_{\text{SZ}} \psi \in H_{\Gamma_0}^1(\Omega)$, the continuity of the normal trace of $\epsilon \mathbf{u}$ and the fact that $\widehat{\epsilon \mathbf{u}_h^n}$ is a single-valued function. We also used the fact that $\Pi_{\text{SZ}} \psi - \psi = 0$ on $\mathcal{E}_{\text{QP}} \cup \mathcal{E}_0$. By the Cauchy-Schwarz inequality, the definition of $\llbracket \cdot \rrbracket_{\text{QP}}$ and the approximation properties of the Scott-Zhang projector in Lemma 3, it follows that

$$\begin{aligned} |(\epsilon(\mathbf{u} - \mathbf{u}_h), \nabla \psi)_{\mathcal{T}_h}| &\leq |(\nabla \cdot \epsilon(\mathbf{u}_h), \psi - \Pi_{\text{SZ}} \psi)_{\mathcal{T}_h}| + |\langle \epsilon(\mathbf{u} - \mathbf{u}_h) \cdot \mathbf{n}, \psi - \Pi_{\text{SZ}} \psi \rangle_{\partial \mathcal{T}_h \setminus (\mathcal{E}_{\text{QP}} \cup \mathcal{E}_0)}| \\ &\quad + |\langle (\epsilon \mathbf{u} - \widehat{\epsilon \mathbf{u}_h^n}) \cdot \mathbf{n}, \Pi_{\text{SZ}} \psi - \psi \rangle_{\mathcal{E}_{\text{QP}}}| + |\langle (\epsilon \mathbf{u} - \widehat{\epsilon \mathbf{u}_h^n}) \cdot \mathbf{n}, \psi \rangle_{\mathcal{E}_{\text{QP}}}| \\ &\leq \|\nabla \cdot \epsilon(\mathbf{u}_h)\|_{\mathcal{T}_h} \|\psi - \Pi_{\text{SZ}} \psi\|_{\mathcal{T}_h} + \|\epsilon(\mathbf{u} - \mathbf{u}_h) \cdot \mathbf{n}\|_{\partial \mathcal{T}_h \setminus (\mathcal{E}_{\text{QP}} \cup \mathcal{E}_0)} \|\psi - \Pi_{\text{SZ}} \psi\|_{\partial \mathcal{T}_h} \\ &\quad + \left\| \llbracket (\epsilon \mathbf{u} - \widehat{\epsilon \mathbf{u}_h^n}) \cdot \mathbf{n} \rrbracket_{\text{QP}} \right\|_{\mathcal{E}_{\text{QP}}} \|\llbracket \psi \rrbracket_{\text{QP}}\|_{\mathcal{E}_{\text{QP}}} \\ &\lesssim (h \|\nabla \cdot \epsilon(\mathbf{u}_h)\|_{\mathcal{T}_h} + h^{1/2} \|\epsilon(\mathbf{u} - \mathbf{u}_h) \cdot \mathbf{n}\|_{\partial \mathcal{T}_h \setminus (\mathcal{E}_{\text{QP}} \cup \mathcal{E}_0)}) |\psi|_{1, \Omega} \\ &\lesssim (h \|\nabla \cdot \epsilon(\mathbf{u}_h)\|_{\mathcal{T}_h} + h^{1/2} \|\llbracket \epsilon(\mathbf{u} - \mathbf{u}_h) \cdot \mathbf{n} \rrbracket_{\mathcal{E}_I}\|) |\psi|_{1, \Omega}, \end{aligned} \tag{20}$$

where we have made use of the fact that $[[\psi]]_{QP} = 0$ because $\psi \in H_{\Gamma_0}^{1,QP}(\Omega)$. Taking into account that $\epsilon \mathbf{u} \in H(\text{div}; \Omega)$, $\widehat{\epsilon \mathbf{u}}_h^n$ is single-valued and (4h), we have

$$\begin{aligned} \|[(\epsilon(\mathbf{u} - \mathbf{u}_h) \cdot \mathbf{n})]\|_{\mathcal{E}_I} &= \|[(\epsilon \mathbf{u}_h - \widehat{\epsilon \mathbf{u}}_h^n) \cdot \mathbf{n}]\|_{\mathcal{E}_I} = \sum_{F \in \mathcal{E}_I} \|[(\epsilon \mathbf{u}_h - \widehat{\epsilon \mathbf{u}}_h^n) \cdot \mathbf{n}]\|_F \\ &= \sum_{F \in \mathcal{E}_I} \|[\tau_n(p_h - \widehat{p}_h)]\|_F \leq \|\tau_n(p_h - \widehat{p}_h)\|_{\partial \mathcal{T}_h}. \end{aligned} \tag{21}$$

Recalling that $\nabla \cdot (\epsilon \mathbf{u}) = 0$, taking $q := \nabla \cdot (\epsilon \mathbf{u}_h)$ in (19), by using the Cauchy-Schwarz inequality, the discrete trace inequality and (4h), there holds

$$\begin{aligned} \|\nabla \cdot (\epsilon \mathbf{u}_h)\|_{\mathcal{T}_h}^2 &= \langle (\epsilon \mathbf{u}_h - \widehat{\epsilon \mathbf{u}}_h^n) \cdot \mathbf{n}, \nabla \cdot (\epsilon \mathbf{u}_h) \rangle_{\partial \mathcal{T}_h} \leq \|(\epsilon \mathbf{u}_h - \widehat{\epsilon \mathbf{u}}_h^n) \cdot \mathbf{n}\|_{\partial \mathcal{T}_h} \|\nabla \cdot (\epsilon \mathbf{u}_h)\|_{\partial \mathcal{T}_h} \\ &\leq \|(\epsilon \mathbf{u}_h - \widehat{\epsilon \mathbf{u}}_h^n) \cdot \mathbf{n}\|_{\partial \mathcal{T}_h} h^{-1/2} \|\nabla \cdot (\epsilon \mathbf{u}_h)\|_{\mathcal{T}_h} \leq h^{-1/2} \|\tau_n(p_h - \widehat{p}_h)\|_{\partial \mathcal{T}_h} \|\nabla \cdot (\epsilon \mathbf{u}_h)\|_{\mathcal{T}_h} \end{aligned}$$

thus

$$\|\nabla \cdot (\epsilon \mathbf{u}_h)\|_{\mathcal{T}_h} \lesssim h^{-1/2} \|\tau_n(p_h - \widehat{p}_h)\|_{\partial \mathcal{T}_h}. \tag{22}$$

Therefore, by using the Cauchy-Schwarz inequality in (18), from (20), (21), (22) and (13), it follows that

$$\|\nabla \psi\|_{\Omega} \lesssim h^{1/2} \|\tau_n(p_h - \widehat{p}_h)\|_{\partial \mathcal{T}_h} + \|h^{1/2}(\mathbf{u}_h - \widehat{\mathbf{u}}_h^t) \times \mathbf{n}\|_{\partial \mathcal{T}_h}. \tag{23}$$

Finally, (12) follows by combining (14), (15), (23) and (17). □

In the following lemma, let us proceed to obtain a computable upper bound for the L^2 -error of the curl of the electric field and its quasi-periodic approximation.

Lemma 6 *Let $(\mathbf{v}, \mathbf{u}, p) \in H(\text{curl}; \Omega) \times \mathbf{X}_{QP}^{\mathbf{g}} \times H_0^1(\Omega)$ and $(\mathbf{v}_h, \mathbf{u}_h, p_h, \widehat{\mathbf{u}}_h^t, \widehat{p}_h) \in \mathbf{V}_h \times \mathbf{V}_h \times Q_h \times \mathbf{M}_{QP}^{\mathbf{g}} \times M_h$ be the solutions of (2) and (4), respectively. Then,*

$$\begin{aligned} \|\nabla \times (\mathbf{u} - \mathbf{u}_h^{QP})\|_{\mathcal{T}_h} &\lesssim \|h^{-1/2}(\mathbf{u}_h - \widehat{\mathbf{u}}_h^t) \times \mathbf{n}\|_{\partial \mathcal{T}_h} + h^{\ell-1} \sum_{K \in \mathcal{T}_h} \eta_{K,1} + h^{\ell} \|h^{-1/2} \tau(\widehat{\mathbf{u}}_h^t - \mathbf{u}_h^t)\|_{\partial \mathcal{T}_h} \\ &\quad + h^{\ell-1} \sum_{K \in \mathcal{T}_h} \sum_{F \in \partial K} \eta_{F,3} + h^{1/2} \|\tau_n(p_h - \widehat{p}_h)\|_{\partial \mathcal{T}_h} + h^{\ell-1/2} \|p_h - \widehat{p}_h\|_{\partial \mathcal{T}_h} \end{aligned} \tag{24}$$

where \mathbf{u}_h^{QP} is given by Lemma 2 for $\mathbf{u}_h \in \mathbf{V}_h$ and $\ell \in (0, 1)$ such that the continuous embedding

$$H_{\Gamma_{QP}}(\text{div}_\epsilon^0; \Omega) \cap H_{\Gamma_0}(\mathbf{curl}; \Omega) \hookrightarrow \mathbf{H}^\ell(\Omega) \tag{25}$$

holds.

Proof Let $\mathbf{u}_h^{QP} \in \mathbf{V}_h^c$ be the quasi-periodic approximation of \mathbf{u}_h with $\mathbf{u}_h^{QP} \times \mathbf{n}|_{\Gamma_0} = \mathbf{g}$ provided in Lemma 2. Let us consider the Helmholtz decomposition of $\mathbf{u} - \mathbf{u}_h^{QP} \in \mathbf{L}^2(\Omega)$ (Appendix A.1):

$$\mathbf{u} - \mathbf{u}_h^{QP} = \nabla\varphi + \mathbf{v}_s, \tag{26}$$

with $\|\mathbf{u} - \mathbf{u}_h^{QP}\|_\Omega^2 = \|\nabla\varphi\|^2 + \|\mathbf{v}_s\|^2$, where $\varphi \in H_{\Gamma_0}^1(\Omega)$ and $\mathbf{v}_s \in H_{\Gamma_{QP}}(\text{div}_\epsilon^0; \Omega)$. In addition, since $(\mathbf{u} - \mathbf{u}_h^{QP}) \times \mathbf{n} = \mathbf{0}$ on Γ_0 and $\nabla\varphi \times \mathbf{n}|_{\Gamma_0} = \mathbf{curl}|_{\Gamma_0}\varphi = \mathbf{0}$, we conclude that $\mathbf{v}_s \in H_{\Gamma_0}(\mathbf{curl}; \Omega)$. Thus, for $\mathbf{v}_s \in H_{\Gamma_{QP}}(\text{div}_\epsilon^0; \Omega) \cap H_{\Gamma_0}(\mathbf{curl}; \Omega)$ there exists $\ell \in (0, 1)$ such that $\mathbf{v}_s \in \mathbf{H}^\ell(\Omega)$ and $\|\mathbf{v}_s\|_{\ell, \Omega} \lesssim \|\mathbf{v}_s\|_{H(\mathbf{curl}; \Omega)}$, thanks the continuous embedding $H_{\Gamma_{QP}}(\text{div}_\epsilon^0; \Omega) \cap H_{\Gamma_0}(\mathbf{curl}; \Omega) \hookrightarrow \mathbf{H}^\ell(\Omega)$ (see Remark 8.7 in [21]).

Then, adding and subtracting \mathbf{u}_h , it follows that

$$\begin{aligned} \|\nabla \times (\mathbf{u} - \mathbf{u}_h^{QP})\|_{\mathcal{T}_h}^2 &= (\nabla \times (\mathbf{u} - \mathbf{u}_h^{QP}), \nabla \times (\nabla\varphi + \mathbf{v}_s))_{\mathcal{T}_h} \\ &= (\nabla \times (\mathbf{u} - \mathbf{u}_h), \nabla \times \mathbf{v}_s)_{\mathcal{T}_h} + (\nabla \times (\mathbf{u}_h - \mathbf{u}_h^{QP}), \nabla \times \mathbf{v}_s)_{\mathcal{T}_h}. \end{aligned}$$

For the second term, according to (7d), we have that

$$\begin{aligned} (\nabla \times (\mathbf{u}_h - \mathbf{u}_h^{QP}), \nabla \times \mathbf{v}_s)_{\mathcal{T}_h} &\leq \|\nabla \times (\mathbf{u}_h - \mathbf{u}_h^{QP})\|_{\mathcal{T}_h} \|\nabla \times \mathbf{v}_s\|_{\mathcal{T}_h} \\ &\lesssim \left(\|h^{-1/2} \llbracket \mathbf{u}_h \rrbracket \|_{\mathcal{E}_I} + \|h^{-1/2} \llbracket \mathbf{u}_h \rrbracket_{QP} \|_{\mathcal{E}_{QP}} + \|h^{-1/2} (\mathbf{u}_h \times \mathbf{n} - \mathbf{g}) \|_{\mathcal{E}_0} \right) \|\nabla \times \mathbf{v}_s\|_{\mathcal{T}_h} \\ &\lesssim \|h^{-1/2} (\mathbf{u}_h - \widehat{\mathbf{u}}_h^t) \times \mathbf{n}\|_{\partial\mathcal{T}_h} \|\nabla \times \mathbf{v}_s\|_{\mathcal{T}_h}, \end{aligned} \tag{27}$$

where in the last step, we have used the facts that $\llbracket \widehat{\mathbf{u}}_h^t \rrbracket = 0$ on \mathcal{E}_I , $\llbracket \widehat{\mathbf{u}}_h^t \rrbracket_{QP} = 0$ on \mathcal{E}_{QP} (Remark 1) and $\widehat{\mathbf{u}}_h^t \times \mathbf{n} = \mathbf{g}$ on Γ_0 . Thus, since $\nabla \times \mathbf{v}_s = \nabla \times (\mathbf{u} - \mathbf{u}_h^{QP})$ and apply the Young inequality, as follows

$$\|\nabla \times (\mathbf{u} - \mathbf{u}_h^{QP})\|_{\mathcal{T}_h}^2 \lesssim (\nabla \times (\mathbf{u} - \mathbf{u}_h), \nabla \times \mathbf{v}_s)_{\mathcal{T}_h} + \|h^{-1/2} (\mathbf{u}_h - \widehat{\mathbf{u}}_h^t) \times \mathbf{n}\|_{\partial\mathcal{T}_h}^2. \tag{28}$$

Now, if we use the \mathbf{L}^2 -projector over $\mathbf{P}_0(\mathcal{T}_h)$, $\Pi_{\mathbf{V}}^0$ (see [35]), in the first term of (28), apply the Green’s identity of $H(\mathbf{curl}; \mathcal{T}_h)$, use (2a) and (2b), it follows that

$$\begin{aligned} &(\nabla \times (\mathbf{u} - \mathbf{u}_h), \nabla \times \mathbf{v}_s)_{\mathcal{T}_h} \\ &= (\nabla \times (\mathbf{u} - \mathbf{u}_h), \nabla \times (\mathbf{v}_s - \Pi_{\mathbf{V}}^0 \mathbf{v}_s))_{\mathcal{T}_h} \\ &= (\nabla \times \nabla \times (\mathbf{u} - \mathbf{u}_h), \mathbf{v}_s - \Pi_{\mathbf{V}}^0 \mathbf{v}_s)_{\mathcal{T}_h} \\ &\quad - \langle (\nabla \times (\mathbf{u} - \mathbf{u}_h))^t, (\mathbf{v}_s - \Pi_{\mathbf{V}}^0 \mathbf{v}_s) \times \mathbf{n} \rangle_{\partial\mathcal{T}_h} \\ &= (\mathbf{f} - \bar{\epsilon} \nabla p + \kappa^2 \epsilon \mathbf{u} - \nabla \times \nabla \times \mathbf{u}_h, \mathbf{v}_s - \Pi_{\mathbf{V}}^0 \mathbf{v}_s)_{\mathcal{T}_h} \\ &\quad - \langle (\mathbf{v} - \nabla \times \mathbf{u}_h)^t, (\mathbf{v}_s - \Pi_{\mathbf{V}}^0 \mathbf{v}_s) \times \mathbf{n} \rangle_{\partial\mathcal{T}_h}. \end{aligned} \tag{29}$$

Now, by taking $\mathbf{z} := \Pi_{\mathbf{V}}^0 \mathbf{v}_s$ in (10) and applying the Green’s identity of $H(\text{div}; \mathcal{T}_h)$ to the fourth term of the obtained equation, we have

$$\begin{aligned} 0 &= (\mathbf{v} - \mathbf{v}_h, \nabla \times \Pi_{\mathbf{V}}^0 \mathbf{v}_s)_{\mathcal{T}_h} + \langle \mathbf{v}^t - \widehat{\mathbf{v}}_h^t, \Pi_{\mathbf{V}}^0 \mathbf{v}_s \times \mathbf{n} \rangle_{\partial\mathcal{T}_h} - \kappa^2 (\epsilon (\mathbf{u} - \mathbf{u}_h), \Pi_{\mathbf{V}}^0 \mathbf{v}_s)_{\mathcal{T}_h} \\ &\quad - (p - p_h, \nabla \cdot (\epsilon \Pi_{\mathbf{V}}^0 \mathbf{v}_s))_{\mathcal{T}_h} + \langle p - \widehat{p}_h, \epsilon \Pi_{\mathbf{V}}^0 \mathbf{v}_s \cdot \mathbf{n} \rangle_{\partial\mathcal{T}_h}, \end{aligned}$$

from which,

$$0 = \langle \mathbf{v}^t - \widehat{\mathbf{v}}_h^t, \Pi_{\mathbf{V}}^0 \mathbf{v}_s \times \mathbf{n} \rangle_{\partial \mathcal{T}_h} - \kappa^2 \langle \epsilon(\mathbf{u} - \mathbf{u}_h), \Pi_{\mathbf{V}}^0 \mathbf{v}_s \rangle_{\mathcal{T}_h} + \langle p - \widehat{p}_h, \epsilon \Pi_{\mathbf{V}}^0 \mathbf{v}_s \cdot \mathbf{n} \rangle_{\partial \mathcal{T}_h}, \tag{30}$$

thanks to the fact that ϵ is a piecewise constant. Then, by using (30), let us rewrite the second term on the right hand side of (29), thus

$$\begin{aligned} & \langle (\mathbf{v} - \nabla \times \mathbf{u}_h)^t, (\mathbf{v}_s - \Pi_{\mathbf{V}}^0 \mathbf{v}_s) \times \mathbf{n} \rangle_{\partial \mathcal{T}_h} \\ &= \langle \mathbf{v}^t, \mathbf{v}_s \times \mathbf{n} \rangle_{\partial \mathcal{T}_h} - \langle \mathbf{v}^t, \Pi_{\mathbf{V}}^0 \mathbf{v}_s \times \mathbf{n} \rangle_{\partial \mathcal{T}_h} - \langle (\nabla \times \mathbf{u}_h)^t, (\mathbf{v}_s - \Pi_{\mathbf{V}}^0 \mathbf{v}_s) \times \mathbf{n} \rangle_{\partial \mathcal{T}_h} \\ &= \langle \mathbf{v}^t, \mathbf{v}_s \times \mathbf{n} \rangle_{\partial \mathcal{T}_h} - \langle \widehat{\mathbf{v}}_h^t, \Pi_{\mathbf{V}}^0 \mathbf{v}_s \times \mathbf{n} \rangle_{\partial \mathcal{T}_h} - \kappa^2 \langle \epsilon(\mathbf{u} - \mathbf{u}_h), \Pi_{\mathbf{V}}^0 \mathbf{v}_s \rangle_{\mathcal{T}_h} \\ & \quad + \langle p - \widehat{p}_h, \epsilon \Pi_{\mathbf{V}}^0 \mathbf{v}_s \cdot \mathbf{n} \rangle_{\partial \mathcal{T}_h} - \langle (\nabla \times \mathbf{u}_h)^t, (\mathbf{v}_s - \Pi_{\mathbf{V}}^0 \mathbf{v}_s) \times \mathbf{n} \rangle_{\partial \mathcal{T}_h}. \end{aligned}$$

Let us note that the first term on the right hand side vanishes, since $\mathbf{v}_s \in H_{\Gamma_0}(\mathbf{curl}; \Omega)$, \mathbf{u}_h^{QP} and φ satisfies quasi-periodic conditions. In fact, by using the definitions of \mathbf{v} [cf. (2a)] and \mathbf{v}_s [cf. (26)], we have that

$$\begin{aligned} \langle \mathbf{v}^t, \mathbf{v}_s \times \mathbf{n} \rangle_{\partial \mathcal{T}_h} &= \langle \mathbf{v}^t, \mathbf{v}_s \times \mathbf{n} \rangle_{\partial \mathcal{T}_h \setminus \Gamma} + \langle \mathbf{v}^t, \mathbf{v}_s \times \mathbf{n} \rangle_{\Gamma_0} + \langle \mathbf{v}^t, \mathbf{v}_s \times \mathbf{n} \rangle_{\Gamma_{\text{QP}}} \\ &= \langle \mathbf{v}^t, \mathbf{v}_s \times \mathbf{n} \rangle_{\Gamma_{\text{QP}}} = \langle (\nabla \times \mathbf{u})^t, \mathbf{v}_s \times \mathbf{n} \rangle_{\Gamma_{\text{QP}}} \\ &= \langle (\nabla \times \mathbf{u})^t, (\mathbf{u} - \mathbf{u}_h^{\text{QP}}) \times \mathbf{n} \rangle_{\Gamma_{\text{QP}}} - \langle (\nabla \times \mathbf{u})^t, \nabla \varphi \times \mathbf{n} \rangle_{\Gamma_{\text{QP}}} \\ &= \langle (\nabla \times \mathbf{u})^t, (\mathbf{u} - \mathbf{u}_h^{\text{QP}}) \times \mathbf{n} \rangle_{\Gamma_1 \cup \Gamma_2} + \langle (\nabla \times \mathbf{u})^t, (\mathbf{u} - \mathbf{u}_h^{\text{QP}}) \times \mathbf{n} \rangle_{\Gamma_3 \cup \Gamma_4} \\ &= \langle (\nabla \times \mathbf{u})^t, (\mathbf{u} - \mathbf{u}_h^{\text{QP}}) \times \mathbf{n} \rangle_{\Gamma_1} - |e^{i\alpha L}| \langle (\nabla \times \mathbf{u})^t, (\mathbf{u} - \mathbf{u}_h^{\text{QP}}) \times \mathbf{n} \rangle_{\Gamma_1} \\ & \quad + \langle (\nabla \times \mathbf{u})^t, (\mathbf{u} - \mathbf{u}_h^{\text{QP}}) \times \mathbf{n} \rangle_{\Gamma_3} - |e^{i\beta L}| \langle (\nabla \times \mathbf{u})^t, (\mathbf{u} - \mathbf{u}_h^{\text{QP}}) \times \mathbf{n} \rangle_{\Gamma_3} = 0. \end{aligned}$$

In addition, if we add $0 = \langle \widehat{\mathbf{v}}_h^t, \mathbf{v}_s \times \mathbf{n} \rangle_{\partial \mathcal{T}_h}$ in the second term, it is obtained that

$$\begin{aligned} & \langle (\mathbf{v} - \nabla \times \mathbf{u}_h)^t, (\mathbf{v}_s - \Pi_{\mathbf{V}}^0 \mathbf{v}_s) \times \mathbf{n} \rangle_{\partial \mathcal{T}_h} = - \langle \widehat{\mathbf{v}}_h^t, (\Pi_{\mathbf{V}}^0 \mathbf{v}_s - \mathbf{v}_s) \times \mathbf{n} \rangle_{\partial \mathcal{T}_h} \\ & - \kappa^2 \langle \epsilon(\mathbf{u} - \mathbf{u}_h), \Pi_{\mathbf{V}}^0 \mathbf{v}_s \rangle_{\mathcal{T}_h} + \langle p - \widehat{p}_h, \epsilon \Pi_{\mathbf{V}}^0 \mathbf{v}_s \cdot \mathbf{n} \rangle_{\partial \mathcal{T}_h} - \langle (\nabla \times \mathbf{u}_h)^t, (\mathbf{v}_s - \Pi_{\mathbf{V}}^0 \mathbf{v}_s) \times \mathbf{n} \rangle_{\partial \mathcal{T}_h}. \end{aligned}$$

Then, after replacing the above expression in (29), add $0 = \langle p - \widehat{p}_h, \epsilon \mathbf{v}_s \cdot \mathbf{n} \rangle_{\partial \mathcal{T}_h}$ and by adding and subtracting $\kappa^2 \epsilon \mathbf{u}_h$ and $\bar{\epsilon} \nabla p_h$ in the first term, we can form the residual associated to (2b), as follows

$$\begin{aligned} \langle \nabla \times (\mathbf{u} - \mathbf{u}_h), \nabla \times \mathbf{v}_s \rangle_{\mathcal{T}_h} &= (\mathbf{f} - \bar{\epsilon} \nabla p_h + \kappa^2 \epsilon \mathbf{u}_h - \nabla \times \nabla \times \mathbf{u}_h, \mathbf{v}_s - \Pi_{\mathbf{V}}^0 \mathbf{v}_s)_{\mathcal{T}_h} \\ & \quad - \kappa^2 \langle \epsilon(\mathbf{u} - \mathbf{u}_h), \mathbf{v}_s \rangle_{\mathcal{T}_h} \\ & \quad - \langle \widehat{\mathbf{v}}_h^t - (\nabla \times \mathbf{u}_h)^t, (\mathbf{v}_s - \Pi_{\mathbf{V}}^0 \mathbf{v}_s) \times \mathbf{n} \rangle_{\partial \mathcal{T}_h} \\ & \quad + \langle p - \widehat{p}_h, \epsilon (\mathbf{v}_s - \Pi_{\mathbf{V}}^0 \mathbf{v}_s) \cdot \mathbf{n} \rangle_{\partial \mathcal{T}_h} \\ & \quad - \langle \nabla(p - p_h), \epsilon (\mathbf{v}_s - \Pi_{\mathbf{V}}^0 \mathbf{v}_s) \rangle_{\mathcal{T}_h}, \end{aligned}$$

using Green's identity and recalling that $\epsilon(\mathbf{v}_s - \Pi_{\mathbf{V}}^0 \mathbf{v}_s)$ is divergence free on each element, it is obtained that

$$\begin{aligned} \langle \nabla \times (\mathbf{u} - \mathbf{u}_h), \nabla \times \mathbf{v}_s \rangle_{\mathcal{T}_h} &= (\mathbf{f} - \bar{\epsilon} \nabla p_h + \kappa^2 \epsilon \mathbf{u}_h + \nabla \times \nabla \times \mathbf{u}_h, \mathbf{v}_s - \Pi_{\mathbf{V}}^0 \mathbf{v}_s)_{\mathcal{T}_h} \\ & \quad - \kappa^2 \langle \epsilon(\mathbf{u} - \mathbf{u}_h), \mathbf{v}_s \rangle_{\mathcal{T}_h} \\ & \quad - \langle \widehat{\mathbf{v}}_h^t - (\nabla \times \mathbf{u}_h)^t, (\mathbf{v}_s - \Pi_{\mathbf{V}}^0 \mathbf{v}_s) \times \mathbf{n} \rangle_{\partial \mathcal{T}_h} \\ & \quad + \langle p_h - \widehat{p}_h, \epsilon (\mathbf{v}_s - \Pi_{\mathbf{V}}^0 \mathbf{v}_s) \cdot \mathbf{n} \rangle_{\partial \mathcal{T}_h} \end{aligned}$$

Now, if we use (26) to rewrite \mathbf{v}_s in the second term, adding and subtracting \mathbf{v}_h^t in the third term and taking account the numerical flux (4h), it holds

$$\begin{aligned}
 (\nabla \times (\mathbf{u} - \mathbf{u}_h), \nabla \times \mathbf{v}_s)_{\mathcal{T}_h} &= (\mathbf{f} - \bar{\epsilon} \nabla p_h + \kappa^2 \epsilon \mathbf{u}_h - \nabla \times \nabla \times \mathbf{u}_h, \mathbf{v}_s - \Pi_{\mathbf{V}}^0 \mathbf{v}_s)_{\mathcal{T}_h} \\
 &\quad - \kappa^2 (\epsilon (\mathbf{u} - \mathbf{u}_h), \mathbf{u} - \mathbf{u}_h^{\text{QP}})_{\mathcal{T}_h} \\
 &\quad + \kappa^2 (\epsilon (\mathbf{u} - \mathbf{u}_h), \nabla \varphi)_{\mathcal{T}_h} + \langle p_h - \hat{p}_h, \epsilon (\mathbf{v}_s - \Pi_{\mathbf{V}}^0 \mathbf{v}_s) \cdot \mathbf{n} \rangle_{\partial \mathcal{T}_h} \\
 &\quad + \langle \tau (\hat{\mathbf{u}}_h^t - \mathbf{u}_h^t), \mathbf{v}_s - \Pi_{\mathbf{V}}^0 \mathbf{v}_s \rangle_{\partial \mathcal{T}_h} \\
 &\quad + \langle \mathbf{v}_h^t - (\nabla \times \mathbf{u}_h)^t, (\mathbf{v}_s - \Pi_{\mathbf{V}}^0 \mathbf{v}_s) \times \mathbf{n} \rangle_{\partial \mathcal{T}_h}.
 \end{aligned}$$

Since $-\kappa^2 (\epsilon (\mathbf{u} - \mathbf{u}_h), \mathbf{u} - \mathbf{u}_h^{\text{QP}})_{\mathcal{T}_h} = -\kappa^2 \|\epsilon^{1/2} (\mathbf{u} - \mathbf{u}_h)\|_{\mathcal{T}_h}^2 - \kappa^2 (\epsilon (\mathbf{u} - \mathbf{u}_h), \mathbf{u}_h - \mathbf{u}_h^{\text{QP}})_{\mathcal{T}_h}$, from the above equality we obtain that

$$\begin{aligned}
 &\kappa^2 \|\epsilon^{1/2} (\mathbf{u} - \mathbf{u}_h)\|_{\mathcal{T}_h}^2 + (\nabla \times (\mathbf{u} - \mathbf{u}_h), \nabla \times \mathbf{v}_s)_{\mathcal{T}_h} \\
 &= (\mathbf{f} - \bar{\epsilon} \nabla p_h + \kappa^2 \epsilon \mathbf{u}_h - \nabla \times \nabla \times \mathbf{u}_h, \mathbf{v}_s - \Pi_{\mathbf{V}}^0 \mathbf{v}_s)_{\mathcal{T}_h} \\
 &\quad - \kappa^2 (\epsilon (\mathbf{u} - \mathbf{u}_h), \mathbf{u}_h - \mathbf{u}_h^{\text{QP}})_{\mathcal{T}_h} \\
 &\quad + \kappa^2 (\epsilon (\mathbf{u} - \mathbf{u}_h), \nabla \varphi)_{\mathcal{T}_h} + \langle p_h - \hat{p}_h, \epsilon (\mathbf{v}_s - \Pi_{\mathbf{V}}^0 \mathbf{v}_s) \cdot \mathbf{n} \rangle_{\partial \mathcal{T}_h} \\
 &\quad + \langle \tau (\hat{\mathbf{u}}_h^t - \mathbf{u}_h^t), \mathbf{v}_s - \Pi_{\mathbf{V}}^0 \mathbf{v}_s \rangle_{\partial \mathcal{T}_h} + \langle \mathbf{v}_h^t - (\nabla \times \mathbf{u}_h)^t, (\mathbf{v}_s - \Pi_{\mathbf{V}}^0 \mathbf{v}_s) \times \mathbf{n} \rangle_{\partial \mathcal{T}_h}.
 \end{aligned} \tag{31}$$

In what follows, we bound each term on the right hand side of (31), by applying the Cauchy-Schwarz inequality, the definitions of the error indicators (6a), (6e), the relation (4g), the approximation properties of $\Pi_{\mathbf{V}}^0$ and the inverse inequality, we have

★:

$$\begin{aligned}
 (\mathbf{f} - \bar{\epsilon} \nabla p_h + \kappa^2 \epsilon \mathbf{u}_h - \nabla \times \nabla \times \mathbf{u}_h, \mathbf{v}_s - \Pi_{\mathbf{V}}^0 \mathbf{v}_s)_{\mathcal{T}_h} &\leq \sum_{K \in \mathcal{T}_h} h_K^{-1} \eta_{K,1} \|\mathbf{v}_s - \Pi_{\mathbf{V}}^0 \mathbf{v}_s\|_K \\
 &\lesssim \sum_{K \in \mathcal{T}_h} h_K^{-1} \eta_{K,1} h_K^\ell \|\mathbf{v}_s\|_{\ell,K} \\
 &\leq h^{\ell-1} \|\mathbf{v}_s\|_{\ell,\Omega} \sum_{K \in \mathcal{T}_h} \eta_{K,1},
 \end{aligned}$$

★:

$$\langle \tau (\hat{\mathbf{u}}_h^t - \mathbf{u}_h^t), \mathbf{v}_s - \Pi_{\mathbf{V}}^0 \mathbf{v}_s \rangle_{\partial \mathcal{T}_h} \lesssim h^\ell \|\mathbf{v}_s\|_{\ell,\Omega} \|h^{-1/2} \tau (\hat{\mathbf{u}}_h^t - \mathbf{u}_h^t)\|_{\partial \mathcal{T}_h}$$

★:

$$\begin{aligned}
 \langle \mathbf{v}_h^t - (\nabla \times \mathbf{u}_h)^t, (\mathbf{v}_s - \Pi_{\mathbf{V}}^0 \mathbf{v}_s) \times \mathbf{n} \rangle_{\partial \mathcal{T}_h} &= \langle \mathbf{n} \times (\mathbf{v}_h - \nabla \times \mathbf{u}_h), \mathbf{v}_s - \Pi_{\mathbf{V}}^0 \mathbf{v}_s \rangle_{\partial \mathcal{T}_h} \\
 &\leq \sum_{K \in \mathcal{T}_h} \|\mathbf{n} \times (\mathbf{v}_h - \nabla \times \mathbf{u}_h)\|_{\partial K} \|\mathbf{v}_s - \Pi_{\mathbf{V}}^0 \mathbf{v}_s\|_{\partial K} \\
 &\leq \sum_{K \in \mathcal{T}_h} \|\mathbf{n} \times (\mathbf{v}_h - \nabla \times \mathbf{u}_h)\|_{\partial K} h_K^{-1/2} \|\mathbf{v}_s - \Pi_{\mathbf{V}}^0 \mathbf{v}_s\|_K \\
 &\lesssim \sum_{K \in \mathcal{T}_h} \left(h_K^{\ell-1/2} \|\mathbf{v}_s\|_{\ell,K} \sum_{F \in \partial K} \|\mathbf{n} \times (\mathbf{v}_h - \nabla \times \mathbf{u}_h)\|_F \right) \\
 &\leq \sum_{K \in \mathcal{T}_h} \left(h_K^{\ell-1/2} \|\mathbf{v}_s\|_{\ell,K} \sum_{F \in \partial K} h_F^{-1/2} \eta_{F,3} \right) \\
 &\lesssim h^{\ell-1} \|\mathbf{v}_s\|_{\ell,\Omega} \sum_{K \in \mathcal{T}_h} \sum_{F \in \partial K} \eta_{F,3}
 \end{aligned}$$

★:

$$\begin{aligned} \langle \epsilon(\mathbf{u} - \mathbf{u}_h), \mathbf{u}_h - \mathbf{u}_h^{\text{QP}} \rangle_{\mathcal{T}_h} &\leq \|\epsilon(\mathbf{u} - \mathbf{u}_h)\|_{\mathcal{T}_h} \|\mathbf{u}_h - \mathbf{u}_h^{\text{QP}}\|_{\mathcal{T}_h} \\ &\lesssim h^{1/2} \|\epsilon(\mathbf{u} - \mathbf{u}_h)\|_{\mathcal{T}_h} \|(\mathbf{u}_h - \widehat{\mathbf{u}}_h^t) \times \mathbf{n}\|_{\partial\mathcal{T}_h}, \end{aligned}$$

★:

$$\langle \epsilon(\Pi_V^0 \mathbf{v}_s \cdot \mathbf{n} - \mathbf{v}_s \cdot \mathbf{n}), p_h - \widehat{p}_h \rangle_{\partial\mathcal{T}_h} \lesssim h^{\ell-1/2} \|\mathbf{v}_s\|_{\ell,\Omega} \|p_h - \widehat{p}_h\|_{\partial\mathcal{T}_h}.$$

★:

$$\begin{aligned} \langle \epsilon(\mathbf{u} - \mathbf{u}_h), \nabla\varphi \rangle_{\mathcal{T}_h} &\leq \|\epsilon(\mathbf{u} - \mathbf{u}_h)\|_{\mathcal{T}_h} \|\nabla\varphi\|_{\mathcal{T}_h} \\ &\lesssim \|\epsilon(\mathbf{u} - \mathbf{u}_h)\|_{\mathcal{T}_h} (h^{1/2} \|\tau_n(p_h - \widehat{p}_h)\|_{\partial\mathcal{T}_h} + \|h^{1/2}(\mathbf{u}_h - \widehat{\mathbf{u}}_h^t) \times \mathbf{n}\|_{\partial\mathcal{T}_h}), \end{aligned}$$

Where in the last inequality, we have used (23) for ψ in place of φ . Using Young’s inequality in the above equations and replacing in (31), we get

$$\begin{aligned} \kappa^2 \|\epsilon(\mathbf{u} - \mathbf{u}_h)\|_{\mathcal{T}_h}^2 + \langle \nabla \times (\mathbf{u} - \mathbf{u}_h), \nabla \times \mathbf{v}_s \rangle_{\mathcal{T}_h} &\lesssim \delta^2 \|\epsilon(\mathbf{u} - \mathbf{u}_h)\|_{\mathcal{T}_h}^2 + \left(h^{\ell-1} \sum_{K \in \mathcal{T}_h} \eta_{K,1} \right)^2 \\ &+ \left(h^\ell \|h^{-1/2} \tau(\widehat{\mathbf{u}}_h^t - \mathbf{u}_h^t)\|_{\partial\mathcal{T}_h} \right)^2 + \left(h^{\ell-1} \sum_{K \in \mathcal{T}_h} \sum_{F \in \partial K} \eta_{F,3} \right)^2 \\ &+ \left(h^{1/2} \|\tau_n(p_h - \widehat{p}_h)\|_{\partial\mathcal{T}_h} \right)^2 \\ &+ \left(\|h^{1/2}(\mathbf{u}_h - \widehat{\mathbf{u}}_h^t) \times \mathbf{n}\|_{\partial\mathcal{T}_h} \right)^2 + \left(h^{\ell-1/2} \|p_h - \widehat{p}_h\|_{\partial\mathcal{T}_h} \right)^2 + \|\mathbf{v}_s\|_{\ell,\Omega}^2. \end{aligned}$$

According with the continuous embedding, we rewrite \mathbf{v}_s by using (26) and (23), we have

$$\begin{aligned} \|\mathbf{v}_s\|_{\ell,\Omega}^2 &\lesssim \|\mathbf{v}_s\|_{\Omega}^2 + \|\nabla \times \mathbf{v}_s\|_{\Omega}^2 = \|\mathbf{u} - \mathbf{u}_h^{\text{QP}} - \nabla\varphi\|_{\mathcal{T}_h}^2 + \|\nabla \times (\mathbf{u} - \mathbf{u}_h^{\text{QP}})\|_{\mathcal{T}_h}^2 \\ &\lesssim \|\nabla\varphi\|_{\Omega}^2 + \|\mathbf{u} - \mathbf{u}_h^{\text{QP}}\|_{\mathcal{T}_h}^2 + \|\nabla \times (\mathbf{u} - \mathbf{u}_h^{\text{QP}})\|_{\mathcal{T}_h}^2 \\ &\lesssim (h^{1/2} \|\tau_n(p_h - \widehat{p}_h)\|_{\partial\mathcal{T}_h})^2 + (\|h^{1/2}(\mathbf{u}_h - \widehat{\mathbf{u}}_h^t) \times \mathbf{n}\|_{\partial\mathcal{T}_h})^2 \\ &+ \|\epsilon(\mathbf{u} - \mathbf{u}_h)\|_{\mathcal{T}_h}^2 + \|\epsilon(\mathbf{u}_h - \mathbf{u}_h^{\text{QP}})\|_{\mathcal{T}_h}^2 + \|\nabla \times (\mathbf{u} - \mathbf{u}_h^{\text{QP}})\|_{\mathcal{T}_h}^2 \\ &\lesssim (h^{1/2} \|\tau_n(p_h - \widehat{p}_h)\|_{\partial\mathcal{T}_h})^2 + (\|h^{1/2}(\mathbf{u}_h - \widehat{\mathbf{u}}_h^t) \times \mathbf{n}\|_{\partial\mathcal{T}_h})^2 + \|\epsilon(\mathbf{u} - \mathbf{u}_h)\|_{\mathcal{T}_h}^2 \\ &+ \|\nabla \times (\mathbf{u} - \mathbf{u}_h^{\text{QP}})\|_{\mathcal{T}_h}^2 \end{aligned}$$

thus

$$\begin{aligned} \|\epsilon(\mathbf{u} - \mathbf{u}_h)\|_{\mathcal{T}_h}^2 + \langle \nabla \times (\mathbf{u} - \mathbf{u}_h), \nabla \times \mathbf{v}_s \rangle_{\mathcal{T}_h} &\lesssim \delta^2 \|\epsilon(\mathbf{u} - \mathbf{u}_h)\|_{\mathcal{T}_h}^2 \\ &+ \left(h^{\ell-1} \sum_{K \in \mathcal{T}_h} \eta_{K,1} \right)^2 + \left(h^\ell \|h^{-1/2} \tau(\widehat{\mathbf{u}}_h^t - \mathbf{u}_h^t)\|_{\partial\mathcal{T}_h} \right)^2 \\ &+ \left(h^{\ell-1} \sum_{K \in \mathcal{T}_h} \sum_{F \in \partial K} \eta_{F,3} \right)^2 + \left(h^{1/2} \|\tau_n(p_h - \widehat{p}_h)\|_{\partial\mathcal{T}_h} \right)^2 \\ &+ (\|h^{1/2}(\mathbf{u}_h - \widehat{\mathbf{u}}_h^t) \times \mathbf{n}\|_{\partial\mathcal{T}_h})^2 \\ &+ \left(h^{\ell-1/2} \|p_h - \widehat{p}_h\|_{\partial\mathcal{T}_h} \right)^2 + \|\nabla \times (\mathbf{u} - \mathbf{u}_h^{\text{QP}})\|_{\mathcal{T}_h}^2. \end{aligned}$$

Finally, replacing in (28), we conclude

$$\begin{aligned} \|\nabla \times (\mathbf{u} - \mathbf{u}_h^{\text{QP}})\|_{\mathcal{T}_h}^2 &\lesssim h^{-1/2}(\mathbf{u}_h - \widehat{\mathbf{u}}_h^t) \times \mathbf{n}\|_{\partial\mathcal{T}_h}^2 + \left(h^{\ell-1} \sum_{K \in \mathcal{T}_h} \eta_{K,1} \right)^2 \\ &\quad + \left(h^\ell \|h^{-1/2} \tau(\widehat{\mathbf{u}}_h^t - \mathbf{u}_h^t)\|_{\partial\mathcal{T}_h} \right)^2 \\ &\quad + \left(h^{\ell-1} \sum_{K \in \mathcal{T}_h} \sum_{F \in \partial K} \eta_{F,3} \right)^2 + (h^{1/2} \|\tau_n(p_h - \widehat{p}_h)\|_{\partial\mathcal{T}_h})^2 \\ &\quad + (\|h^{1/2}(\mathbf{u}_h - \widehat{\mathbf{u}}_h^t) \times \mathbf{n}\|_{\partial\mathcal{T}_h})^2 + (h^{\ell-1/2} \|p_h - \widehat{p}_h\|_{\partial\mathcal{T}_h})^2 \\ &\quad + \widehat{\delta}^2 \|\epsilon(\mathbf{u} - \mathbf{u}_h)\|_{\mathcal{T}_h}^2. \end{aligned}$$

Then, choosing $\widehat{\delta}$ small enough and using the fact that $0 < h < 1$, (24) is deduced from the last inequality. \square

Lemma 7 *Let $(\mathbf{v}, \mathbf{u}, p) \in H(\text{curl}; \Omega) \times \mathbf{X}_{\text{QP}}^{\mathbf{g}} \times H_0^1(\Omega)$ and $(\mathbf{v}_h, \mathbf{u}_h, p_h, \widehat{\mathbf{u}}_h^t, \widehat{p}_h) \in \mathbf{V}_h \times \mathbf{V}_h \times Q_h \times \mathbf{M}_{\text{QP}}^{\mathbf{g}} \times M_h$ be the solutions of (2) and (4), respectively. There holds*

$$\|\nabla \times \mathbf{u}_h - \mathbf{v}_h\|_{\mathcal{T}_h} \lesssim h^{-1/2} \|(\mathbf{u}_h^t - \widehat{\mathbf{u}}_h^t) \times \mathbf{n}\|_{\partial\mathcal{T}_h}. \tag{32}$$

Proof By testing (2a) with \mathbf{w} , apply the Green’s identity and subtracting (4a), we obtain the next error equation

$$(\mathbf{v} - \mathbf{v}_h, \mathbf{w}) - (\mathbf{u} - \mathbf{u}_h, \nabla \times \mathbf{w})_{\mathcal{T}_h} - (\mathbf{u}^t - \widehat{\mathbf{u}}_h^t, \mathbf{w} \times \mathbf{n})_{\partial\mathcal{T}_h} = 0 \quad \forall \mathbf{w} \in \mathbf{V}_h$$

apply the Green’s identity to the second term and using again (2a), it follows

$$\begin{aligned} (\mathbf{v} - \mathbf{v}_h, \mathbf{w})_{\mathcal{T}_h} - (\nabla \times (\mathbf{u} - \mathbf{u}_h), \mathbf{w})_{\mathcal{T}_h} + \langle (\mathbf{u} - \mathbf{u}_h)^t, \mathbf{w} \times \mathbf{n} \rangle_{\partial\mathcal{T}_h} - \langle \mathbf{u}^t - \widehat{\mathbf{u}}_h^t, \mathbf{w} \times \mathbf{n} \rangle_{\partial\mathcal{T}_h} &= 0 \\ (\nabla \times \mathbf{u}_h - \mathbf{v}_h, \mathbf{w})_{\mathcal{T}_h} - \langle (\mathbf{u}_h^t - \widehat{\mathbf{u}}_h^t) \times \mathbf{n}, \mathbf{w} \rangle_{\partial\mathcal{T}_h} &= 0. \end{aligned}$$

Afterwards, by defining $\mathbf{w} := \nabla \times \mathbf{u}_h - \mathbf{v}_h$, applying the Cauchy-Schwarz inequality and the inverse inequality ([18], Lemma 1.46), we obtain (32). \square

Finally, gathering together all the previous results, we deduce the following upper bound for the error in terms of the error estimator and the index ℓ appearing in the continuous embedding (25).

Corollary 2 *Let $(\mathbf{v}, \mathbf{u}, p) \in H(\text{curl}; \Omega) \times \mathbf{X}_{\text{QP}}^{\mathbf{g}} \times H_0^1(\Omega)$ and $(\mathbf{v}_h, \mathbf{u}_h, p_h, \widehat{\mathbf{u}}_h^t, \widehat{p}_h) \in \mathbf{V}_h \times \mathbf{V}_h \times Q_h \times \mathbf{M}_{\text{QP}}^{\mathbf{g}} \times M_h$ be the solutions of 2 and 4, respectively. If the stabilization parameters satisfy $|\tau|$ and $|\tau_n|$ to be proportional to one, then*

$$E_h \lesssim h^{\ell-1} \eta_1 + \eta_2 + h^\ell \eta_1^\partial + \eta_2^\partial + h^{\ell-1} \eta_3^\partial + \eta_4^\partial,$$

where the terms on the right hand side have the following form $\eta_1 := \sum_{K \in \mathcal{T}_h} \eta_{K,1}$, $\eta_2 := \sum_{K \in \mathcal{T}_h} \eta_{K,2}$, $\eta_1^\partial := \sum_{K \in \mathcal{T}_h} \sum_{F \in \partial K} \eta_{F,1}$, $\eta_2^\partial := \sum_{K \in \mathcal{T}_h} \sum_{F \in \partial K} \eta_{F,2}$, $\eta_3^\partial := \sum_{K \in \mathcal{T}_h} \sum_{F \in \partial K} \eta_{F,3}$ and $\eta_4^\partial := \sum_{F \in \mathcal{E}_I \setminus \Gamma} \eta_{F,4}$.

The above estimates imply that error estimator is reliable, i.e., $E_h \lesssim \eta$ when $\ell = 1$. This happens, for instance, when $\Gamma = \Gamma_0$ (see for instance Section 3.4 [22]). In our setting Γ is the union of two disjoint sets Γ_{QP} and Γ_0 , therefore it is not possible to guarantee $\ell = 1$ in (25). However, the numerical experiments in Sect. 5 suggest that the estimator is still reliable even in this case.

4.2 Local Efficiency

In this section we want to study whether or not our a posteriori error estimator shows local efficiency, based on the techniques devised by Verfürth, applying some properties of the bubble functions. Given an element K , a bubble function is defined as $B_K := (d + 1)^{d+1} \prod_{i=1}^{d+1} \lambda_i$, where λ_i is a linear nodal function in the i vertex of K . Hence, $\text{supp}(B_K) \subset K$, $B_K = 0$ on ∂K and $B_K \in [0, 1]$. If the function is built on a face F , then $B_F := d^d \prod_{i=1}^d \lambda_i$, for i vertex of F . In this case, $\text{supp}(B_F) \subset \{K \in \mathcal{T}_h : F \subset \partial K\}$, $B_F = 0$ on $\partial K \setminus F$ and $B_F \in [0, 1]$. Now, let us introduce the properties of the bubble functions, which were proved in [2], Theorems 2.2 and 2.4.

Lemma 8 For given $K \in \mathcal{T}_h$, $F \subset \partial K$, $\phi \in \mathbb{P}(K)$ and $\psi \in \mathbb{P}(F)$, it holds

$$\begin{aligned} C^{-1} \|\phi\|_K^2 &\leq \|B_K^{1/2} \phi\|_K^2 \leq C \|\phi\|_K^2, \\ C^{-1} \|\psi\|_F^2 &\leq \|B_F^{1/2} \psi\|_F^2 \leq C \|\psi\|_F^2, \\ C \|\psi\|_F^2 &\leq \|B_F^{1/2} \mathcal{L}(\psi)\|_K^2 \leq C \|\psi\|_F^2, \end{aligned}$$

where $\mathcal{L} : \mathcal{C}(F) \rightarrow \mathcal{C}(K)$, $\mathcal{L}(\varphi) \in \mathbb{P}(K)$ and $\mathcal{L}(\varphi)|_F = \varphi$, for all $\varphi \in \mathbb{P}(F)$.

In the following Lemma we will employ the properties stated in Lemma 8, in order to study the efficiency of our estimator.

Lemma 9 For all $K \in \mathcal{T}_h$, it holds

$$\eta_{K,1} \lesssim \text{osc}(\mathbf{f}, K) + \|p - p_h\|_K + \kappa^2 h_K \|\epsilon(\mathbf{u} - \mathbf{u}_h)\|_K + \|\nabla \times (\mathbf{u} - \mathbf{u}_h)\|_K, \tag{33a}$$

$$\eta_{K,2} \lesssim \text{osc}(\nabla \cdot \mathbf{f}, K) + \|\nabla(p - p_h)\|_K + \kappa^2 \|\epsilon(\mathbf{u} - \mathbf{u}_h)\|_K. \tag{33b}$$

Proof If we define $R_h := \mathbf{f} - \bar{\epsilon} \nabla p_h + \kappa^2 \epsilon \mathbf{u}_h - \nabla \times \nabla \times \mathbf{u}_h$, the proof follows the same steps as the proof of Lemma 6.4 in [13]. □

Lemma 10 For all $K \in \mathcal{T}_h$ and $F \in \partial K$, there holds

$$\eta_{F,3} \lesssim \|\mathbf{v}_h - \nabla \times \mathbf{u}_h\|_K.$$

Proof The bound is deduced by the definition of $\eta_{F,3}$ and the discrete trace inequality. □

Lemma 11 For all $F \in \mathcal{E}_I$, there holds

$$\begin{aligned} \eta_{F,4} &\lesssim \text{osc}(\nabla \cdot \mathbf{f}, \omega_F) + \text{osc}(\mathbf{f}, \omega_F) \\ &\quad + \kappa^2 \|\epsilon(\mathbf{u} - \mathbf{u}_h)\|_{\omega_F} + \kappa^2 h_{\omega_F} \|\tau_n(p_h - \hat{p}_h)\|_{\partial \omega_F} + \|\nabla(p - p_h)\|_{\omega_F} \end{aligned}$$

where $\omega_F := \cup\{K \in \mathcal{T}_h : \bar{K} \cap \bar{F} \neq \emptyset\}$.

Proof Let $F \in \mathcal{E}_I$, for a given $w \in H_0^1(\omega_F)$, we consider the product between $\left[\left[\bar{\epsilon} \frac{\partial p_h}{\partial \mathbf{n}} \right] \right]$ and w . Then, after applying integration by parts and using the divergence of (2b), we obtain that

$$\begin{aligned} \left\langle \left[\left[\bar{\epsilon} \frac{\partial p_h}{\partial \mathbf{n}} \right] \right], w \right\rangle_F &= (\nabla \cdot \mathbf{f} - \Pi_Q \nabla \cdot \mathbf{f}, w)_{\omega_F} + (\Pi_Q (\nabla \cdot \mathbf{f} + \kappa^2 \nabla \cdot (\epsilon \mathbf{u}_h)) - \nabla \cdot (\bar{\epsilon} \nabla p_h), w)_{\omega_F} \\ &\quad - \kappa^2 (\nabla \cdot (\epsilon \mathbf{u}_h), w)_{\omega_F} + (\bar{\epsilon} \nabla(p - p_h), \nabla w)_{\omega_F}, \end{aligned}$$

from which, using the Lemma 8, the properties of the extension operator \mathcal{L} , choosing $w := B_F \mathcal{L} \left(\left[\bar{\epsilon} \frac{\partial p_h}{\partial \mathbf{n}} \right] \right)$, applying Cauchy-Schwarz inequality and inverse inequality it follows that

$$\begin{aligned} \left\| \left[\bar{\epsilon} \frac{\partial p_h}{\partial \mathbf{n}} \right] \right\|_F^2 &\lesssim (\|\nabla \cdot \mathbf{f} - \Pi_Q \nabla \cdot \mathbf{f}\|_{\omega_F} + \|\Pi_Q(\nabla \cdot \mathbf{f} + \kappa^2 \nabla \cdot (\epsilon \mathbf{u}_h) - \nabla \cdot (\bar{\epsilon} \nabla p_h))\|_{\omega_F} \\ &\quad + \kappa^2 \|\nabla \cdot (\bar{\epsilon} \nabla p_h)\|_{\omega_F} + h_{\omega_F}^{-1} \|\bar{\epsilon} \nabla(p - p_h)\|_{\omega_F}) \left\| B_F \mathcal{L} \left(\left[\bar{\epsilon} \frac{\partial p_h}{\partial \mathbf{n}} \right] \right) \right\|_{\omega_F} \end{aligned}$$

where, by using the Lemma 8 again, we get

$$\left\| B_F \mathcal{L} \left(\left[\bar{\epsilon} \frac{\partial p_h}{\partial \mathbf{n}} \right] \right) \right\|_{\omega_F} \lesssim h_F^{1/2} \left\| \left[\bar{\epsilon} \frac{\partial p_h}{\partial \mathbf{n}} \right] \right\|_F.$$

Thus, from (22)

$$\begin{aligned} h_F^{1/2} \left\| \left[\bar{\epsilon} \frac{\partial p_h}{\partial \mathbf{n}} \right] \right\|_F &\lesssim h_F \|\nabla \cdot \mathbf{f} - \Pi_Q \nabla \cdot \mathbf{f}\|_{\omega_F} + h_F \|\nabla \cdot \mathbf{f} + \kappa^2 \nabla \cdot (\epsilon \mathbf{u}_h) - \nabla \cdot (\bar{\epsilon} \nabla p_h)\|_{\omega_F} \\ &\quad + \kappa^2 h_F^{1/2} h_{\omega_F}^{1/2} \|\tau_n(p_h - \hat{p}_h)\|_{\partial \omega_F} + h_F^{1/2} h_{\omega_F}^{-1/2} \|\bar{\epsilon} \nabla(p - p_h)\|_{\omega_F}. \end{aligned}$$

Hence, we conclude the proof from definitions of $\eta_{F,4}$, $\eta_{K,2}$ and from (33b). \square

Proof of Theorem 1 It follows from Corollary 2, Lemmas 9 and 11.

5 Numerical Results

The numerical experiments were carry out by adapting the routines that we used for the implementation of the proposed HDG method in [10].

The stabilization parameters are set to be $\tau = -i$, $\tau_n = i$ in all the experiments and therefore, a rate of convergence of order h^{k+1} in the L^2 norm is expected for smooth solutions.

For an unknown $w \in \{\mathbf{v}, \mathbf{u}, p\}$ the experimental order of convergence is defined as

$$r(w) = -3 \frac{\|w - w_{h_1}\|_{\Omega} / \|w - w_{h_2}\|_{\Omega}}{N_1 / N_2}, \tag{34}$$

where N_1 and N_2 are the number of elements of two consecutive meshes of sizes h_1 and h_2 ($h_1 > h_2$), respectively. In the same way we define the experimental order of convergence $r(E_h)$ for the global error E_h [cf. (5)]. In addition, we recall the global contribution of each of the local error indicators specified in (6), as follows

$$\begin{aligned} \eta_1 &:= \left(\sum_{K \in \mathcal{T}_h} \eta_{K,1}^2 \right)^{1/2}, & \eta_2 &:= \left(\sum_{K \in \mathcal{T}_h} \eta_{K,2}^2 \right)^{1/2}, & \eta_1^\partial &:= \left(\sum_{K \in \mathcal{T}_h} \sum_{F \in \partial K} \eta_{F,1}^2 \right)^{1/2}, \\ \eta_2^\partial &:= \left(\sum_{K \in \mathcal{T}_h} \sum_{F \in \partial K} \eta_{F,2}^2 \right)^{1/2}, & \eta_3^\partial &:= \left(\sum_{K \in \mathcal{T}_h} \sum_{F \in \partial K} \eta_{F,3}^2 \right)^{1/2}, & \eta_4^\partial &:= \left(\sum_{F \in \mathcal{E}_I} \eta_{F,4}^2 \right)^{1/2}. \end{aligned}$$

Their respective experimental order of convergence are defined as in (34), where now the error estimator takes the place of the error.

Table 1 Rate of convergence and errors of Example 1 with $\tau = -i$ and $\tau_n = i$

k	Nelts	$\ \mathbf{v} - \mathbf{v}_h\ _{\mathcal{T}_h}$	$\ \mathbf{u} - \mathbf{u}_h\ _{\mathcal{T}_h}$	$\ p - p_h\ _{\mathcal{T}_h}$	$r(\mathbf{v})$	$r(\mathbf{u})$	$r(p)$	E_h	$r(E_h)$
1	48	8.99e-01	3.72e-01	2.23e-02	-	-	-	8.38e+00	-
	384	2.88e-01	1.08e-01	6.42e-03	1.64	1.79	1.79	4.56e+00	0.88
	3072	7.84e-02	2.83e-02	1.71e-03	1.88	1.93	1.91	2.30e+00	0.99
	24,576	2.02e-02	7.15e-03	4.46e-04	1.96	1.98	1.94	1.14e+00	1.01
2	48	1.77e-01	6.50e-02	5.12e-03	-	-	-	1.86e+00	-
	384	2.49e-02	9.04e-03	5.51e-04	2.83	2.84	3.22	4.81e-01	1.95
	3072	3.21e-03	1.14e-03	6.97e-05	2.96	2.99	2.98	1.18e-01	2.02
3	48	1.28e-02	6.15e-03	4.96e-04	-	-	-	2.25e-01	-
	384	1.01e-03	4.56e-04	3.06e-05	3.67	3.75	4.02	3.23e-02	2.80
	3072	6.74e-05	3.03e-05	2.02e-06	3.90	3.91	3.92	4.18e-03	2.95

Error estimator and its rate of convergence

5.1 Uniform Refinement

Example 1 We consider a unit cube $\Omega := [0, 1]^3$ divided in two regions $\Omega_d := [0, 1] \times [0, 1] \times [1/2, 1]$ and $\Omega_m := [0, 1] \times [0, 1] \times [0, 1/2]$, which are discretized by a sequence of quasi-uniform tetrahedral meshes. Each element of the meshes satisfies that its interior belongs to either Ω_d or Ω_m . Based on [19], we choose the wavelength $\lambda_0 := 4.5$ (450 nm) and recall that $\kappa := 2\pi/\lambda_0$, that is, $\kappa = 1.3963$. Moreover, we use the following values for the relative electric permittivities, $\epsilon_d := 2.7124$ and $\epsilon_m := -5.8828 + i 0.6650$, which corresponds to the silicon oxynitride and evaporated silver, respectively. We consider the exact solution $\mathbf{u}(x, y, z) := (0, u_2(x, y, z), 0)^T$, where

$$u_2(x, y, z) := \begin{cases} \exp(-i\kappa\sqrt{\epsilon_d}(z - 0.5)) + \exp(i\kappa\sqrt{\epsilon_d}(z - 0.5)), & \text{if } z \geq 0.5, \\ \exp(-i\kappa\sqrt{\epsilon_m}(z - 0.5)) + \exp(i\kappa\sqrt{\epsilon_m}(z - 0.5)), & \text{if } z < 0.5, \end{cases}$$

assume that $p(x, y, z) := 0$ and calculate the values of \mathbf{f} and \mathbf{g} , taking into account the exact solution. We impose quasi-periodic boundary conditions on the vertical walls.

Example 2 In this example we also consider a unit cube $\Omega := [0, 1]^3$ but take as exact solution the quasi-periodic function

$$u_2(x, y, z) := \exp(-i[\kappa_x x + \kappa_y y - \kappa_z(z - 1)]),$$

with $\kappa_x := \kappa \sin \theta \cos \phi$, $\kappa_y := \kappa \sin \theta \sin \phi$, $\kappa_z := (\kappa^2 - \kappa_x^2 - \kappa_y^2)^{1/2}$, $\theta := \pi/3$ and $\phi := \pi$. The boundary conditions on the vertical walls are of quasi-periodic type.

In the history of convergence displayed in Tables 1 and 4, it is observed a rate of convergence of $k + 1$ for the both unknowns, \mathbf{u} and \mathbf{v} , which is better than the predicted results in the Corollary 1. Moreover, we include the error of the a posteriori error estimator and its associated rate of convergence, which tends to the expected order k .

The error indicators and their rates of convergence appear in Tables 2, 3, 5 and 6. As we pointed out before, in this case the continuous embedding (25) holds true for $\ell \in (0, 1)$, therefore Corollary 2 cannot guarantee reliability of the estimator. However, the effectivity index, $\text{eff} := \eta/E_h$ reported included in Tables 3 and 6 remains bounded for each polynomial degree.

Table 2 Rate of convergence and errors of the boundary terms of the error estimator of Example 1 with $\tau = -i$ and $\tau_n = i$

k	Nelts	η_1^{∂}	η_2^{∂}	η_3^{∂}	η_4^{∂}	$r(\eta_1^{\partial})$	$r(\eta_2^{\partial})$	$r(\eta_3^{\partial})$	$r(\eta_4^{\partial})$
1	48	2.43e+00	2.62e-01	1.41e+01	1.23e+00	-	-	-	-
	384	1.43e+00	1.61e-01	7.78e+00	6.55e-01	0.76	0.70	0.86	0.91
	3072	7.58e-01	8.70e-02	4.00e+00	3.15e-01	0.92	0.89	0.96	1.06
	24,576	3.86e-01	4.50e-02	2.01e+00	1.52e-01	0.97	0.95	0.99	1.05
2	48	4.72e-01	5.21e-02	3.76e+00	6.65e-01	-	-	-	-
	384	1.33e-01	1.39e-02	1.02e+00	1.89e-01	1.83	1.90	1.88	1.81
	3072	3.43e-02	3.70e-03	2.54e-01	5.23e-02	1.96	1.91	2.01	1.85
3	48	4.49e-02	6.04e-03	6.49e-01	1.65e-01	-	-	-	-
	384	6.89e-03	8.83e-04	9.60e-02	2.70e-02	2.70	2.77	2.76	2.61
	3072	9.13e-04	1.19e-04	1.26e-02	3.75e-03	2.91	2.89	2.93	2.85

Table 3 Rate of convergence and errors of the volumetric terms of the error estimator of Example 1 with $\tau = -i$ and $\tau_n = i$

k	Nelts	η_1	η_2	$r(\eta_1)$	$r(\eta_2)$	η	$r(\eta)$	eff
1	48	7.37e+00	9.87e-02	-	-	1.62e+01	-	1.93
	384	3.76e+00	2.53e-02	0.97	1.96	8.79e+00	0.88	1.93
	3072	1.89e+00	6.68e-03	1.00	1.92	4.50e+00	0.97	1.96
	24,576	9.43e-01	1.70e-03	1.00	1.97	2.26e+00	0.99	1.98
2	48	3.08e+00	8.23e-01	-	-	4.99e+00	-	2.68
	384	8.55e-01	2.63e-01	1.85	1.64	1.38e+00	1.86	2.87
	3072	2.17e-01	7.26e-02	1.98	1.86	3.48e-01	1.99	2.94
3	48	8.24e-01	3.07e-01	-	-	1.11e+00	-	4.92
	384	1.19e-01	5.55e-02	2.79	2.47	1.65e-01	2.74	5.12
	3072	1.56e-02	7.72e-03	2.94	2.85	2.18e-02	2.92	5.22

Effectivity index associated to the error estimator

Table 4 Rate of convergence and errors of Example 2 with $\tau = -i$ and $\tau_n = i$

k	Nelts	$\ \mathbf{v} - \mathbf{v}_h\ _{\mathcal{T}_h}$	$\ \mathbf{u} - \mathbf{u}_h\ _{\mathcal{T}_h}$	$\ p - p_h\ _{\mathcal{T}_h}$	$r(\mathbf{v})$	$r(\mathbf{u})$	$r(p)$	E_h	$r(E_h)$
1	48	1.37e-01	2.37e-01	7.38e-02	-	-	-	7.49e+00	-
	384	4.06e-02	1.02e-01	3.49e-02	1.76	1.22	1.08	5.23e+00	0.52
	3072	8.00e-03	2.98e-02	7.42e-03	2.34	1.77	2.23	2.84e+00	0.88
	24,576	1.46e-03	8.26e-03	1.31e-03	2.46	1.85	2.50	1.44e+00	0.98
2	48	3.28e-02	8.69e-02	9.18e-02	-	-	-	4.85e+00	-
	384	8.52e-03	3.19e-02	1.76e-02	1.95	1.45	2.38	2.15e+00	1.17
	3072	1.05e-03	4.13e-03	2.35e-03	3.02	2.95	2.91	5.94e-01	1.85
3	48	2.89e-02	7.58e-02	4.86e-02	-	-	-	3.60e+00	-
	384	2.18e-03	6.73e-03	3.88e-03	3.73	3.49	3.65	6.43e-01	2.45
	3072	1.42e-04	4.84e-04	2.66e-04	3.94	3.80	3.87	8.84e-02	2.86

Error estimator and its rate of convergence

Table 5 Rate of convergence and errors of the boundary terms, that appear in the error estimator of Example 2, with $\tau = -i$ and $\tau_n = i$

k	Nelts	η_1^∂	η_2^∂	η_3^∂	η_4^∂	$r(\eta_1^\partial)$	$r(\eta_2^\partial)$	$r(\eta_3^\partial)$	$r(\eta_4^\partial)$
1	48	6.39e-01	8.73e-01	1.90e+00	5.17e+00	-	-	-	-
	384	3.23e-01	8.58e-01	1.01e+00	7.76e+00	0.98	0.03	0.92	-0.59
	3072	1.44e-01	5.23e-01	3.95e-01	4.97e+00	1.17	0.71	1.35	0.64
	24,576	5.61e-02	2.84e-01	1.74e-01	2.74e+00	1.36	0.88	1.18	0.86
2	48	1.94e-01	5.55e-01	1.35e+00	8.83e+00	-	-	-	-
	384	8.99e-02	2.88e-01	7.08e-01	4.59e+00	1.11	0.95	0.93	0.94
	3072	2.52e-02	8.00e-02	2.22e-01	1.22e+00	1.83	1.85	1.68	1.91
3	48	1.73e-01	3.51e-01	2.13e+00	7.16e+00	-	-	-	-
	384	2.60e-02	6.73e-02	3.39e-01	1.73e+00	2.73	2.38	2.65	2.05
	3072	3.64e-03	9.56e-03	4.86e-02	2.50e-01	2.84	2.81	2.80	2.79

Table 6 Rate of convergence and errors of the volumetric terms of the error estimator of Example 2 with $\tau = -i$ and $\tau_n = i$. Effectivity index of the error estimator

k	Nelts	η_1	η_2	$r(\eta_1)$	$r(\eta_2)$	η	$r(\eta)$	eff
1	48	9.57e-01	8.48e+00	-	-	1.02e+01	-	1.36
	384	4.09e-01	5.76e+00	1.23	0.56	9.77e+00	0.07	1.87
	3072	1.58e-01	2.88e+00	1.37	1.00	5.78e+00	0.76	2.04
	24,576	7.05e-02	1.44e+00	1.17	1.00	3.11e+00	0.89	2.15
2	48	1.21e+00	8.81e+00	-	-	1.26e+01	-	2.60
	384	6.19e-01	3.10e+00	0.97	1.51	5.63e+00	1.16	2.62
	3072	2.63e-01	8.29e-01	1.24	1.90	1.52e+00	1.89	2.56
3	48	2.79e+00	7.57e+00	-	-	1.10e+01	-	3.04
	384	5.19e-01	1.38e+00	2.43	2.46	2.30e+00	2.26	3.57
	3072	7.38e-02	1.99e-01	2.81	2.79	3.32e-01	2.79	3.75

5.2 Adaptive Refinement

The adaptive refinement can be carried out following the next steps:

- Solve the variational problem in a coarse mesh.
- Estimate η_K , for each $K \in \mathcal{T}_h$.
- Mark each $\tilde{K} \in \mathcal{T}_h$ such that $\eta_{\tilde{K}} > \theta \max_{K \in \mathcal{T}_h} \eta_K$, for $\theta \in [0, 1]$.
- Refine the coarse mesh and repeat the algorithm until the established stopping criterion allows it. In this step, we use the free library TetGen integrated with MATLAB, see <https://wias-berlin.de/software/tetgen/>.

In the adaptive procedure, the a posteriori error indicators help to identify the elements of a mesh where the errors are bigger than others. Once those parts are found, the algorithm refine them to generate a new refined mesh, as we will illustrate in the following example.

Example 3 (L-shaped domain) With the aim to illustrate the adaptive performance of our HDG scheme, we include an experiment in a L-shaped domain $\Omega := [-1, 1] \times [-1, 1] \times [0, 1] \setminus ([0, 1] \times [-1, 0] \times [0, 1])$ occupied by a material with relative permittivity $\epsilon := 1$.

Fig. 2 Total error E_h versus number of elements N (logarithmic scale) of the approximation of Example 3. Uniform and adaptive refinements

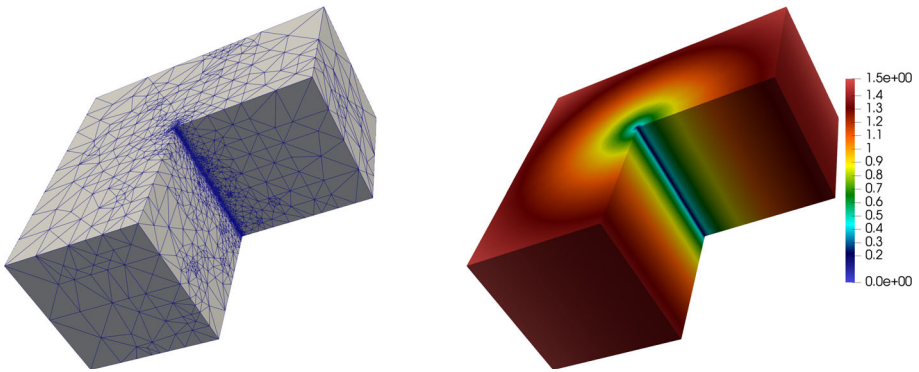
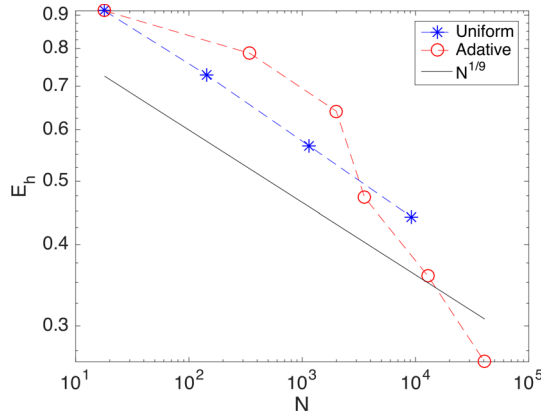


Fig. 3 Approximation of the electric field intensity $|u_h|$ and corresponding adaptive refined mesh of Example 3 with $k = 1$ and $N = 41226$

As in Section 5 of [14], let us consider the exact solution $p(x, y, z) := 0$ and $\mathbf{u}(x, y, z) := \left(\frac{\partial S}{\partial x}, \frac{\partial S}{\partial y}, 0\right)^T$, where $S(r, \theta) := r^{\frac{2n}{3}} \sin\left(\frac{2n\theta}{3}\right)$ is given in terms of cylindrical coordinates (r, θ) and n is a given number. Moreover, as in the above examples, the source term and boundary data were derived from the exact solution. This manufactured solution belongs to $[H^{t-\delta}(\Omega)]^3$ for all $\delta > 0$. The stabilization parameters satisfies $|\tau| = |\tau_n| = 1$ and we choose n such that $\frac{2n}{3} = t$.

The adaptive refinement of our domain was carried out for $k = 1$ and we began with a coarse mesh of 18 elements, in which were marked the tetrahedra \tilde{K} that satisfy the adaptive criterion $\eta_{\tilde{K}} > \theta \max_{K \in \mathcal{T}_h} \eta_K$, for $\theta = 0.1$, in order to refine them.

Figure 2 depicts the obtained errors versus the number of the elements when $t = 1.35$, the meshes are uniformly refined (blue) and by using adaptive criterion (red).

6 Concluding Remarks

In this contribution, we extend our *a priori* error analysis of the HDG method for Maxwell’s equations in heterogeneous media with Dirichlet boundary condition, to a problem with quasi-

periodic boundary conditions on the vertical boundaries of the physical domain. Although, for the real problem it is still necessary to consider transmission conditions on the top and bottom of the cell, the obtained theoretical and numerical results allow us to classify our method as suitable for carrying out the numerical approximation of the solution for this type of boundary value problems (Fig. 3).

With the aim to strengthen our stability estimates, we develop an a posteriori error analysis for the HDG scheme. Based on the confiability and efficiency proofs of the proposed a posteriori error estimator, we decide to corroborate the theoretical results by means of some numerical experiments. In them, we use uniformly refined meshes and depict the history of convergence in some tables.

The performance of the adaptive case was showed for the HDG method proposed for the problem with Dirichlet boundary condition [10]. The behavior of the error can be observed in a graph (Fig. 2), in which it is compared with the obtained error in the case of uniform refinement.

Acknowledgements The first author was supported by COLCIENCIAS through the 647 call. M. Solano was supported by CONICYT-Chile through Grant AFB170001 of the PIA Program: Concurso Apoyo a Centros Científicos y Tecnológicos de Excelencia con Financiamiento Basal and Grant FONDECYT-1160320. M. Solano also acknowledges the support of the MathAmSud project MATH2020010. The second and third authors were supported by the Universidad Nacional de Colombia, Hermes project 34809.

Author Contributions As a convention, the names of the authors are alphabetically order. All authors contributed equally in this article.

Funding Open Access funding provided by Colombia Consortium.

Data Availability The datasets generated during and/or analyzed during the current study are available from the corresponding author on reasonable request.

Declarations

Conflict of interest The authors have no competing interests to declare that are relevant to the content of this article.

Open Access This article is licensed under a Creative Commons Attribution 4.0 International License, which permits use, sharing, adaptation, distribution and reproduction in any medium or format, as long as you give appropriate credit to the original author(s) and the source, provide a link to the Creative Commons licence, and indicate if changes were made. The images or other third party material in this article are included in the article's Creative Commons licence, unless indicated otherwise in a credit line to the material. If material is not included in the article's Creative Commons licence and your intended use is not permitted by statutory regulation or exceeds the permitted use, you will need to obtain permission directly from the copyright holder. To view a copy of this licence, visit <http://creativecommons.org/licenses/by/4.0/>.

A. Appendix

A.1 Helmholtz decomposition

In this appendix we will extend the Helmholtz decomposition given in [21, section 6], for spaces with quasi-periodic conditions. Let us remark that the boundary $\Gamma = \partial\Omega$ is split in two subsets Γ_0 and Γ_{QP} where $\bar{\Gamma}_0$ and $\bar{\Gamma}_{QP}$ are compact Lipschitz submanifold of Γ and Ω is simply connected. Let 3×3 matrix value function ω satisfying the following symmetry,

boundedness and ellipticity conditions

$$\omega_{ij} = \omega_{ji} \in L^\infty(\Omega) \quad i, j = 1, 2, 3, \quad \sum_{i,j=1}^3 \omega_{ij} \xi_i \xi_j \geq \omega_* \|\xi\|^2 \quad \text{a.e. in } \Omega \quad \forall \xi \in \mathbb{R}^3.$$

Proposition 1 *It holds*

$$\mathbf{L}^2(\Omega) = \nabla H_{\Gamma_0}^{1, \text{QP}}(\Omega) \oplus H_{\Gamma_{\text{QP}}}(\text{div}_\omega^0; \Omega)$$

and the subspaces of the right-hand are closed and ω -orthogonal in $\mathbf{L}^2(\Omega)$, where

$$H_{\Gamma_0}^{1, \text{QP}}(\Omega) := \left\{ \psi \in H_{\Gamma_0}^1(\Omega) : \psi|_{\Gamma_2} = e^{i\alpha L} \psi|_{\Gamma_1}, \psi|_{\Gamma_4} = e^{i\beta L} \psi|_{\Gamma_3} \right\}.$$

Proof The proof follows similar lines to those in [21, Proposition 6.1] taking into account that $H_{\Gamma_0}^{1, \text{QP}}(\Omega)$ is a closed subspace of $H^1(\Omega)$. □

A.2 Proof of Lemma 4.1

In this part we present a sketch of the proof of (7c)–(7d), which is included in Lemma 2, by tailoring the arguments employed in the deduction of the properties stated in Proposition 4.5 of [25].

To begin, we recall the definitions of the moments for Nédélec’s elements ([35], Definition 5.30), in a tetrahedron K :

$$\begin{aligned} M_e(\mathbf{w}) &:= \left\{ \int_e (\mathbf{w} \cdot \mathbf{t}_e) \mathbf{q} \, ds : \text{for all } \mathbf{q} \in \mathbf{P}_{k-1}(e) \right\}, \quad \text{for any edge } e \text{ of } K \\ M_F(\mathbf{w}) &:= \left\{ \frac{1}{\text{area}(F)} \int_F (\mathbf{w} \cdot \mathbf{q}) \, dA : \text{for all } \mathbf{q} \in \mathbf{P}_{k-2}(F) \wedge \mathbf{q} \cdot \mathbf{n} = 0 \right\}, \quad \text{for any face } F \text{ of } K, \\ M_K(\mathbf{w}) &:= \left\{ \int_K (\mathbf{w} \cdot \mathbf{q}) \, dV : \text{for all } \mathbf{q} \in \mathbf{P}_{k-3}(K) \right\}, \end{aligned}$$

where \mathbf{t}_e denotes the unit vector in the direction of the edge e . For a given $K \in \mathcal{T}_h$, let $\{\varphi_{K,e}^j\}$, $\{\varphi_{K,F}^j\}$, $\{\varphi_{K,b}^j\}$ the Lagrange basis functions of $\mathbf{P}_k(K)$ with respect to the moments for Nédélec’s elements. Then, there exists $\mathbf{w}^c \in \mathbf{V}_h^c$ that satisfies (7c) and can be decomposed as

$$\mathbf{w}^c|_K = \sum_{e \in \mathcal{L}_h(K)} \sum_{j=1}^{N_e} \alpha_{K,e}^j \varphi_{K,e}^j + \sum_{F \in \mathcal{E}_h(K)} \sum_{j=1}^{N_F} \alpha_{K,F}^j \varphi_{K,F}^j + \sum_{j=1}^{N_b} \alpha_{K,b}^j \varphi_{K,b}^j,$$

where $\mathcal{L}_h(K)$ and $\mathcal{E}_h(K)$ denote the set of edges and faces of K , respectively. Here, N_e , N_F and N_b are the number of basis functions associated to the edges, faces and interior of K , respectively; and $\alpha_{K,e}^j$, $\alpha_{K,F}^j$ and $\alpha_{K,b}^j$ are the coefficients that are uniquely determined.

Based on \mathbf{w}^c , we build a function in \mathbf{V}_h^c that also satisfies quasi-periodic conditions. To that end, we just modify the degrees of freedom associated to the edges and faces that belong to Γ_2 and Γ_4 . More precisely, let $\mathcal{L}_{\Gamma_j}(K)$ and $\mathcal{E}_{\Gamma_j}(K)$ denote the set of edges and faces of K , lying on Γ_j , $j = 1, 2, 3$ and 4 , respectively. We also write $\mathcal{L}_{\text{QP}}(K) := \cup_{j=1}^4 \mathcal{L}_{\Gamma_j}(K)$ and $\mathcal{E}_{\text{QP}}(K) := \cup_{j=1}^4 \mathcal{E}_{\Gamma_j}(K)$. Let us now recall that we are assuming conformity between the discretizations of the periodic boundaries Γ_1 - Γ_2 and Γ_3 - Γ_4 . Therefore, for an edge e_2 (face F_2) belonging to Γ_2 , there is an edge e_1 (face F_1) belonging to Γ_1 “aligned” to e_2 (face F_2).

Similarly for the periodic boundary $\Gamma_3 - \Gamma_4$. On each K such that $\bar{K} \cap \Gamma_{QP} = \emptyset$, we set $\mathbf{w}^{QP} = \mathbf{w}^c$ and, for K such that $\bar{K} \cap \Gamma_{QP} \neq \emptyset$, we set

$$\begin{aligned} \mathbf{w}^{QP}|_K := & \sum_{j=1}^{N_b} \alpha_{K,b}^j \varphi_{K,b}^j + \sum_{e \in \mathcal{L}_h(K) \setminus (\mathcal{L}_{\Gamma_2}(K) \cup \mathcal{L}_{\Gamma_4}(K))} \sum_{j=1}^{N_e} \alpha_{K,e}^j \varphi_{K,e}^j \\ & + \sum_{F \in \mathcal{E}_h(K) \setminus (\mathcal{E}_{\Gamma_2}(K) \cup \mathcal{E}_{\Gamma_4}(K))} \sum_{j=1}^{N_F} \alpha_{K,F} \varphi_{K,F}^j \\ & + \sum_{F_2 \in \mathcal{E}_{\Gamma_2}(K)} \sum_{j=1}^{N_{F_2}} \beta_{K,F_2}^j \varphi_{K,F_2}^j \\ & + \sum_{F_4 \in \mathcal{E}_{\Gamma_4}(K)} \sum_{j=1}^{N_{F_4}} \beta_{K,F_4}^j \varphi_{K,F_4}^j \\ & + \sum_{e_2 \in \mathcal{L}_{\Gamma_2}(K)} \sum_{j=1}^{N_{e_2}} \beta_{K,e_2}^j \varphi_{K,e_2}^j \\ & + \sum_{e_4 \in \mathcal{L}_{\Gamma_4}(K)} \sum_{j=1}^{N_{e_4}} \beta_{K,e_4}^j \varphi_{K,e_4}^j, \end{aligned}$$

where,

$$\beta_{K,F_2}^j := e^{i\alpha L} \alpha_{K',F_1}^j, \quad \beta_{K,e_2}^j := e^{i\alpha L} \alpha_{K',e_1}^j, \quad \beta_{K,F_4}^j := e^{i\beta L} \alpha_{K',F_3}^j, \quad \beta_{K,e_4}^j := e^{i\beta L} \alpha_{K',e_3}^j \tag{35}$$

and K' is the ‘‘neighbor’’ of K across Γ_{QP} .

We notice that $\mathbf{w}^{QP} \in \mathbf{V}_h^c$ since all the degrees of freedom associated to interior edges and faces have remained unchanged. Moreover, the continuity of the Lagrange basis function and the relation (35), between the coefficients, imply that \mathbf{w}^{QP} is quasi-periodic. Hence,

$$\begin{aligned} (\mathbf{w}^c - \mathbf{w}^{QP})|_K = & \sum_{F_2 \in \mathcal{E}_{\Gamma_2}(K)} \sum_{j=1}^{N_{F_2}} (\alpha_{K,F_2}^j - \beta_{K,F_2}^j) \varphi_{K,F_2}^j \\ & + \sum_{F_4 \in \mathcal{E}_{\Gamma_4}(K)} \sum_{j=1}^{N_{F_4}} (\alpha_{K,F_4}^j - \beta_{K,F_4}^j) \varphi_{K,F_4}^j \\ & + \sum_{e_2 \in \mathcal{L}_{\Gamma_2}(K)} \sum_{j=1}^{N_{e_2}} (\alpha_{K,e_2}^j - \beta_{K,e_2}^j) \varphi_{K,e_2}^j \\ & + \sum_{e_4 \in \mathcal{L}_{\Gamma_4}(K)} \sum_{j=1}^{N_{e_4}} (\alpha_{K,e_4}^j - \beta_{K,e_4}^j) \varphi_{K,e_4}^j \end{aligned}$$

and by using (35), we obtain

$$\begin{aligned} \int_K |\mathbf{w}^c - \mathbf{w}^{QP}|^2 &\lesssim h_K \left(\sum_{F_2 \in \mathcal{E}\Gamma_2(K)} \sum_{j=1}^{N_{F_2}} (\alpha_{K,F_2}^j - e^{i\alpha L} \alpha_{K',F_1}^j)^2 \right. \\ &+ \sum_{F_4 \in \mathcal{E}\Gamma_4(K)} \sum_{j=1}^{N_{F_4}} (\alpha_{K,F_4}^j - e^{i\beta L} \alpha_{K',F_3}^j)^2 \\ &+ \sum_{e_2 \in \mathcal{L}\Gamma_2(K)} \sum_{j=1}^{N_{e_2}} (\alpha_{K,e_2}^j - e^{i\alpha L} \alpha_{K',e_1}^j)^2 + \sum_{e_4 \in \mathcal{L}\Gamma_4(K)} \sum_{j=1}^{N_{e_4}} (\alpha_{K,e_4}^j - e^{i\beta L} \beta_{K',e_3}^j)^2 \Big). \end{aligned}$$

Then, taking into account the above estimate and the fact that for a function \mathbf{w} , the tangential trace on a face F is uniquely determined by the degrees of freedom $M_F(\mathbf{w})$ and $M_e(\mathbf{w})$, we have that

$$\begin{aligned} \int_K |\mathbf{w}^c - \mathbf{w}^{QP}|^2 &\lesssim h_K \left(\sum_{F_2 \in \mathcal{E}\Gamma_2(K)} \int_{F_2} |\mathbf{n}^+ \times (\mathbf{w}^c - \mathbf{w}^{QP})|^2 \right. \\ &+ \sum_{F_4 \in \mathcal{E}\Gamma_4(K)} \int_{F_4} |\mathbf{n}^+ \times (\mathbf{w}^c - \mathbf{w}^{QP})|^2 \\ &+ \sum_{e_2 \in \mathcal{L}\Gamma_2(K)} \int_{\mathcal{L}\Gamma_2(K)} |\mathbf{n}^+ \times (\mathbf{w}^c - \mathbf{w}^{QP})|^2 \\ &+ \sum_{e_4 \in \mathcal{L}\Gamma_4(K)} \int_{\mathcal{L}\Gamma_4(K)} |\mathbf{n}^+ \times (\mathbf{w}^c - \mathbf{w}^{QP})|^2 \Big) \\ &\lesssim h_K \left(\sum_{F_2 \in \mathcal{E}\Gamma_2(K)} \int_{F_2} |\mathbf{n}^+ \times \mathbf{w}^c + (\mathbf{n}^- \times e^{i\alpha L} \mathbf{w}^c)|_{K',F_1}|^2 \right. \\ &+ \sum_{F_4 \in \mathcal{E}\Gamma_4(K)} \int_{F_4} |\mathbf{n}^+ \times \mathbf{w}^c + (\mathbf{n}^- \times e^{i\beta L} \mathbf{w}^c)|_{K',F_3}|^2 \\ &+ \sum_{e_2 \in \mathcal{L}\Gamma_2(K)} \int_{e_2} |\mathbf{n}^+ \times \mathbf{w}^c + (\mathbf{n}^- \times e^{i\alpha L} \mathbf{w}^c)|_{K',e_1}|^2 \\ &+ \sum_{e_4 \in \mathcal{L}\Gamma_4(K)} \int_{e_4} |\mathbf{n}^+ \times \mathbf{w}^c + (\mathbf{n}^- \times e^{i\beta L} \mathbf{w}^c)|_{K',e_3}|^2 \Big) \\ &= h_K \left(\sum_{F_2 \in \mathcal{E}\Gamma_2(K)} \int_{F_2} \llbracket \mathbf{w}^c \rrbracket_{QP} + \sum_{F_4 \in \mathcal{E}\Gamma_4(K)} \int_{F_4} \llbracket \mathbf{w}^c \rrbracket_{QP} \right. \\ &+ \sum_{e_2 \in \mathcal{L}\Gamma_2(K)} \int_{e_2} \llbracket \mathbf{w}^c \rrbracket_{e_2} + \sum_{e_4 \in \mathcal{L}\Gamma_4(K)} \int_{e_4} \llbracket \mathbf{w}^c \rrbracket_{e_4} \Big). \end{aligned}$$

Therefore, we deduce that

$$\|\mathbf{w}^c - \mathbf{w}^{QP}\|_{\mathcal{T}_h} \lesssim \|h^{1/2} \llbracket \mathbf{w}^c \rrbracket_{QP}\|_{\Gamma_{QP}} = \|h^{1/2} \llbracket \mathbf{w} \rrbracket_{QP}\|_{\Gamma_{QP}}.$$

The last equality since $\gamma_t(\mathbf{w}) = \gamma_t(\mathbf{w}^c)$ on Γ_{QP} .

Finally, (7c) follows by adding and subtracting $\mathbf{w} \in \mathbf{V}_h$ in $\|\mathbf{w}^c - \mathbf{w}^{\text{QP}}\|_{\mathcal{T}_h}$, applying the triangle inequality together with the above expression and (7a). The estimate (7d) is obtained using the inverse inequality $\|\nabla \times (\mathbf{w} - \mathbf{w}^{\text{QP}})\|_{\mathcal{T}_h} \lesssim h^{-1} \|\mathbf{w} - \mathbf{w}^{\text{QP}}\|_{\mathcal{T}_h}$ and (7c).

References

- Acosta, S., Villamizar, V., Malone, B.: The DtN nonreflecting boundary condition for multiple scattering problems in the half-plane. *Comput. Methods Appl. Mech. Eng.* **217**, 1–11 (2012)
- Ainsworth, M., Oden, J.T.: A posteriori error estimation in finite element analysis. *Comput. Methods Appl. Mech. Eng.* **142**(1–2), 1–88 (1997)
- Araya, R., Solano, M., Vega, P.: Analysis of an adaptive HDG method for the Brinkman problem. *IMA J. Numer. Anal.* **39**(3), 1502–1528 (2018)
- Atwater, H.A., Polman, A.: Plasmonics for improved photovoltaic devices. In: *Materials for Sustainable Energy: A Collection of Peer-Reviewed Research and Review Articles from Nature Publishing Group*, pp. 1–11. World Scientific (2011)
- Bardi, I., Remski, R., Perry, D., Cendes, Z.: Plane wave scattering from frequency-selective surfaces by the finite-element method. *IEEE Trans. Magn.* **38**(2), 641–644 (2002)
- Beck, R., Hiptmair, R., Wohlmuth, B.: Hierarchical error estimator for eddy current computation. In: *Numerical Mathematics and Advanced Applications (Jyväskylä, 1999)*, pp. 110–120 (1999)
- Beck, R., Hiptmair, R., Hoppe, R.H.W., Wohlmuth, B.: Residual based a posteriori error estimators for eddy current computation. *ESAIM Math. Model. Numer. Anal.* **34**(1), 159–182 (2000)
- Berenger, J.-P.: A perfectly matched layer for the absorption of electromagnetic waves. *J. Comput. Phys.* **114**(2), 185–200 (1994)
- Bonito, A., Guermond, J.-L., Luddens, F.: Regularity of the Maxwell equations in heterogeneous media and Lipschitz domains. *J. Math. Anal. Appl.* **408**(2), 498–512 (2013)
- Camargo, L., López-Rodríguez, B., Osorio, M., Solano, M.: An HDG method for Maxwell equations in heterogeneous media. *Comput. Methods Appl. Mech. Eng.* **368**, 113178 (2020)
- Chen, G., Cui, J., Xu, L.: Analysis of hybridizable discontinuous Galerkin finite element method for time-harmonic Maxwell's equations part I: zero frequency. *arXiv preprint arXiv:1805.09291* (2018)
- Chen, H., Li, J., Qiu, W.: Robust a posteriori error estimates for HDG method for convection–diffusion equations. *IMA J. Numer. Anal.* **36**, 437–462 (2016)
- Chen, H., Qiu, W., Shi, K.: A priori and computable a posteriori error estimates for an HDG method for the coercive Maxwell equations. *Comput. Methods Appl. Mech. Eng.* **333**, 287–310 (2018)
- Chen, H., Qiu, W., Shi, K., Solano, M.: A superconvergent HDG method for the Maxwell equations. *J. Sci. Comput.* **70**(3), 1010–1029 (2017)
- Chen, Z., Haijun, W.: An adaptive finite element method with perfectly matched absorbing layers for the wave scattering by periodic structures. *SIAM J. Numer. Anal.* **41**(3), 799–826 (2004)
- Cockburn, B., Zhang, W.: A posteriori error estimates for HDG methods. *J. Sci. Comput.* **51**(3), 582–607 (2012)
- Cockburn, B., Zhang, W.: A posteriori error analysis for hybridizable discontinuous Galerkin methods for second order elliptic problems. *SIAM J. Numer. Anal.* **51**, 676–693 (2013)
- Di Pietro, D.A., Ern, A.: *Mathematical Aspects of Discontinuous Galerkin Methods*, vol. 69. Springer, Berlin (2011)
- Faryad, M., Hall, A.S., Barber, G.D., Mallouk, T.E., Lakhtakia, A.: Excitation of multiple surface-plasmon-polariton waves guided by the periodically corrugated interface of a metal and a periodic multilayered isotropic dielectric material. *J. Opt. Soc. Am. B* **29**(4), 704–713 (2012)
- Feng, X., Peipei, L., Xuejun, X.: A hybridizable discontinuous Galerkin method for the time-harmonic Maxwell equations with high wave number. *Comput. Methods Appl. Math.* **16**(3), 429–445 (2016)
- Fernandes, P., Gilardi, G.: Magnetostatic and electrostatic problems in inhomogeneous anisotropic media with irregular boundary and mixed boundary conditions. *Math. Models Methods Appl. Sci.* **7**(07), 957–991 (1997)
- Girault, V., Raviart, P.-A.: *Finite Element Methods for Navier–Stokes Equations: Theory and Algorithms*, vol. 5. Springer, Berlin (2012)
- Gralak, B.: Exact modal methods. In: Popov, E., (Ed.) *Gratings: Theory and Numeric Applications*, Chapter 10. Université d'Aix-Marseille, Aix Marseille Université, CNRS, Centrale Marseille, Institut Fresnel UMR 7249, Marseille (2014)

24. Gravenkamp, H., Song, C., Prager, J.: A numerical approach for the computation of dispersion relations for plate structures using the scaled boundary finite element method. *J. Sound Vib.* **331**(11), 2543–2557 (2012)
25. Houston, P., Perugia, I., Schneebeli, A., Schötzau, D.: Interior penalty method for the indefinite time-harmonic Maxwell equations. *Numerische Mathematik* **100**(3), 485–518 (2005)
26. Huber, M., Schöberl, J., Sinwel, A., Zaglmayr, S.: Simulation of diffraction in periodic media with a coupled finite element and plane wave approach. *SIAM J. Sci. Comput.* **31**(2), 1500–1517 (2009)
27. Ichikawa, H.: Electromagnetic analysis of diffraction gratings by the finite-difference time-domain method. *J. Opt. Soc. Am. A* **15**(1), 152–157 (1998)
28. Jiang, X., Zhang, L., Zheng, W.: Adaptive hp-finite element computations for time-harmonic Maxwell's equations. *Commun. Comput. Phys.* **13**(2), 559–582 (2013)
29. Karakashian, O.A., Pascal, F.: A posteriori error estimates for a discontinuous Galerkin approximation of second-order elliptic problems. *SIAM J. Numer. Anal.* **41**, 2374–2399 (2003)
30. Karakashian, O.A., Pascal, F.: Convergence of adaptive discontinuous Galerkin approximations of second-order elliptic problems. *SIAM J. Numer. Anal.* **45**(2), 641–665 (2007)
31. Li, J., Lin, Y.: A priori and posteriori error analysis for time-dependent Maxwell's equations. *Comput. Methods Appl. Mech. Eng.* **292**, 54–68 (2015)
32. Maier, S.A.: *Plasmonics: Fundamentals and Applications*. Springer, Berlin (2007)
33. Marly, N., Baekelandt, B., De Zutter, D., Poes, H.F.: Integral equation modeling of the scattering and absorption of multilayered doubly-periodic lossy structures. *IEEE Trans. Antennas Propag.* **43**(11), 1281–1287 (1995)
34. Monk, P.: A posteriori error indicators for Maxwell's equations. *J. Comput. Appl. Math.* **100**(2), 173–190 (1998)
35. Monk, P.: *Finite Element Methods for Maxwell's Equations*. Oxford University Press, Oxford (2003)
36. Monk, P.B., Rivas, C., Rodríguez, R., Solano, M.E.: An asymptotic model based on matching far and near field expansions for thin gratings problems. *ESAIM M2AN* **55**, S507–S533 (2021)
37. Muhammad, F., Lakhtakia, A.: Enhancement of light absorption efficiency of amorphous-silicon thin-film tandem solar cell due to multiple surface-plasmon-polariton waves in the near-infrared spectral regime. *Opt. Eng.* **52**(8), 1–10 (2013)
38. Nguyen, C.T., Tassoulas, J.L.: Reciprocal absorbing boundary condition for the time-domain numerical analysis of wave motion in unbounded layered media. *Proc. R. Soc. A Math. Phys. Eng. Sci.* **473**(2199), 201–60528 (2017)
39. Nguyen, N.C., Peraire, J., Cockburn, B.: Hybridizable discontinuous Galerkin methods for the time-harmonic Maxwell's equations. *J. Comput. Phys.* **230**(19), 7151–7175 (2011)
40. Oswald, P.: On a BPX-preconditioner for P1 elements. *Computing* **51**(2), 125–133 (1993)
41. Rivas, C., Rodríguez, R., Solano, M.E.: A perfectly matched layer for finite-element calculations of diffraction by metallic surface-relief gratings. *Wave Motion* **78**, 68–82 (2018)
42. Rivas, C., Solano, M.E., Rodríguez, R., Monk, P.B., Lakhtakia, A.: Asymptotic Model for Finite-Element Calculations of Diffraction by Shallow Metallic Surface-Relief Gratings
43. Schöberl, J.: A posteriori error estimates for Maxwell equations. *Math. Comput.* **77**(262), 633–649 (2008)
44. Scott, L.R., Zhang, S.: Finite element interpolation of nonsmooth functions satisfying boundary conditions. *Math. Comput.* **54**, 483–493 (1990)
45. Solano, M.E., Barber, G.D., Lakhtakia, A., Faryad, M., Monk, P.B., Mallouk, T.E.: Buffer layer between a planar optical concentrator and a solar cell. *AIP Adv.* **5**(9), 097150 (2015)
46. Solano, M.E., Faryad, M., Monk, P.B., Mallouk, T.E., Lakhtakia, A.: Periodically multilayered planar optical concentrator for photovoltaic solar cells. *Appl. Phys. Lett.* **103**(19), 191115 (2013)
47. Vidal-Codina, F., Nguyen, N.C., Oh, S.-H., Peraire, J.: A hybridizable discontinuous Galerkin method for computing nonlocal electromagnetic effects in three-dimensional metallic nanostructures. *J. Comput. Phys.* **355**, 548–565 (2018)
48. Zhang, D., Ma, F.: A finite element method with perfectly matched absorbing layers for the wave scattering by a periodic chiral structure. *J. Comput. Math.* **66**, 458–472 (2007)